

GEOLOGIC MAP OF THE BRINNON 7.5-MINUTE QUADRANGLE, JEFFERSON AND KITSAP COUNTIES, WASHINGTON

by Michael Polenz, Eleanor Spangler,
Logan A. Fusso, David A. Reieux,
Ryan A. Cole, Timothy J. Walsh,
Recep Cakir, Kenneth P. Clark,
Jeffrey H. Tepper, Robert J. Carson,
Domenico Pileggi, and Shannon A. Mahan

WASHINGTON
DIVISION OF GEOLOGY
AND EARTH RESOURCES
Map Series 2012-02
December 2012



WASHINGTON STATE DEPARTMENT OF
Natural Resources

Peter Goldmark - Commissioner of Public Lands

DISCLAIMER

Neither the State of Washington, nor any agency thereof, nor any of their employees, makes any warranty, express or implied, or assumes any legal liability or responsibility for the accuracy, completeness, or usefulness of any information, apparatus, product, or process disclosed, or represents that its use would not infringe privately owned rights. Reference herein to any specific commercial product, process, or service by trade name, trademark, manufacturer, or otherwise, does not necessarily constitute or imply its endorsement, recommendation, or favoring by the State of Washington or any agency thereof. The views and opinions of authors expressed herein do not necessarily state or reflect those of the State of Washington or any agency thereof.

INDEMNIFICATION

Research supported by the U.S. Geological Survey, National Cooperative Geologic Mapping Program, under USGS award number G11AC20236. The views and conclusions contained in this document are those of the authors and should not be interpreted as necessarily representing the official policies, either expressed or implied, of the U.S. Government.

WASHINGTON STATE DEPARTMENT OF NATURAL RESOURCES

Peter Goldmark—*Commissioner of Public Lands*

DIVISION OF GEOLOGY AND EARTH RESOURCES

David K. Norman—*State Geologist*

John P. Bromley—*Assistant State Geologist*

Washington Department of Natural Resources Division of Geology and Earth Resources

<i>Mailing Address:</i>	<i>Street Address:</i>
MS 47007	Natural Resources Bldg, Rm 148
Olympia, WA 98504-7007	1111 Washington St SE
	Olympia, WA 98501

Phone: 360-902-1450; *Fax:* 360-902-1785

E-mail: geology@dnr.wa.gov

Website: <http://www.dnr.wa.gov/ResearchScience/GeologyEarthSciences/Pages/Home.aspx>

Publications List: <http://www.dnr.wa.gov/ResearchScience/Topics/GeologyPublicationsLibrary/Pages/pubs.aspx>

Washington Geology Library Catalog: <http://www.dnr.wa.gov/ResearchScience/Topics/GeologyPublicationsLibrary/Pages/washbib.aspx>

Washington State Geologic Information Portal:
http://www.dnr.wa.gov/ResearchScience/Topics/GeosciencesData/Pages/geology_portal.aspx

Suggested Citation: Polenz, Michael; Spangler, Eleanor; Fusso, L. A.; Reieux, D. A.; Cole, R. A.; Walsh, T. J.; Cakir, Recep; Clark, K. P.; Tepper, J. H.; Carson, R. J.; Pileggi, Domenico; Mahan, S. A., 2012, Geologic map of the Brinnon 7.5-minute quadrangle, Jefferson and Kitsap Counties, Washington: Washington Division of Geology and Earth Resources Map Series 2012-02, 1 sheet, scale 1:24,000, with 47 p. text.

Published in the United States of America
© 2012 Washington Division of Geology and Earth Resources

Table of Contents

Introduction.....	1
Methods	1
Discussion and Analysis.....	2
Sediment Provenance and Lithology	2
Ice Limit.....	3
Differentiation of Till Deposits	4
Weathering of Till	4
Age of Till.....	5
Ice-dammed Vashon Recessional Lakes	5
Structure.....	6
Description of Map Units.....	7
Quaternary Unconsolidated Deposits.....	7
Holocene Nonglacial Deposits.....	7
Holocene to Post-glacial Pleistocene Nonglacial Deposits.....	8
Pleistocene Glacial and Nonglacial Deposits.....	9
Vashon Drift (northern-sourced).....	9
Pre-Vashon Olympic-sourced Glacial and Nonglacial Deposits, Undivided	12
Pre-Vashon Glacial Deposits	12
Tertiary Sedimentary and Volcanic Bedrock.....	14
Acknowledgments.....	15
References Cited	16
Appendix A. Age Control Data	22
Appendix B. Lithologic and Petrographic Trends Among Sediments.....	28
Appendix C. Relict Lakeshore Levels.....	31
Appendix D. Selected Structural Data: Seismicity, Faults, and Joints	35
Appendix E. Geochemical Data	38

List of Figures

Figure A1. Photo of alluvium of unit Qpu _{op} at date site GD4	22
Figure A2. Lidar shaded-relief map showing ⁴⁰ Ar- ³⁹ Ar date locations from Crescent Formation volcanic rock samples.....	23
Figure B1. Pie chart comparison of field sites in which abundance of northern-sourced clasts was mentioned	28
Figure B2. Graph of lithologic properties vs. abundance (%) based on sediment source	29
Figure C1. Lidar shaded-relief map showing relict lake shore level data points.....	31
Figure C2. Graph of relict lake-shore altitude markers and implied post-glacial land-level changes and tilt-slope angles along Hood Canal	33
Figure C3. Lidar hillshade image with vertical, simulated sun angle, lower Duckabush River valley	34
Figure D1. Lidar shaded-relief map showing earthquake locations, depths, and magnitudes in and near the Brinnon quadrangle (1970–2011).....	35

Figure D2. Photo of subvertical fault exposed south of Rocky Brook in a cutbank along Forest Road 2630	36
Figure D3. Photos of joint control on Fulton Creek channel walls and waterfall surfaces at significant site S33	37
Figure E1. AFM diagram for basalt samples from the Brinnon quadrangle	46
Figure E2. Total alkalis versus silica plot for lava samples from the Brinnon quadrangle	46
Figure E3. Tectonic discrimination diagram for Crescent Formation lavas	47
Figure E4. Plots of Cr and MgO content in volcanic rock samples from the Brinnon quadrangle.....	47

TABLES

Table 1. List of geochemistry sites, geotechnical sites, well sites, significant sites, and age sites	map plate
Table A1. Age-control data from the map area and basalt ^{40}Ar - ^{39}Ar age estimates from a composite stratigraphic section of the Crescent Formation near the Dosewallips River	24
Table A2. Infrared- and optically stimulated luminescence data and age estimates compared to ages suggested by regional radiocarbon data	27
Table B1. Lithologic and petrographic trends in thin sections from Olympic- vs. northern-sourced samples.....	30
Table C1. Elevations of relict lake delta tops and other shoreline markers from Vashon glaciorecessional, ice-dammed lakes	32
Table E1. X-ray fluorescence and loss on ignition analyses for an andesite pebble	38
Table E2. Comparison of XRF results for a Cascades-sourced volcanic pebble and XRF and ICP-MS results for volcanic clasts from Glacier Peak and Possession Drift.....	39
Table E3. New whole-rock chemical analyses for basalt bedrock samples	42

Geologic Map of the Brinnon 7.5-minute Quadrangle, Jefferson and Kitsap Counties, Washington

by Michael Polenz¹, Eleanor Spangler¹, Logan A. Fusso¹, David A. Reiou¹, Ryan A. Cole², Timothy J. Walsh¹, Recep Cakir¹, Kenneth P. Clark³, Jeffrey H. Tepper³, Robert J. Carson⁴, Domenico Pileggi⁵, and Shannon A. Mahan⁶

¹ Washington Division of
Geology and Earth Resources
MS 47007
Olympia, WA 98504-7007

⁵ Department of Earth Sciences
University of Siena
Via Laterina, 8
53100 Siena Italy

⁴ Department of Geology
Whitman College
345 Boyer Ave
Walla Walla, WA 99362

³ Department of Geology
University of Puget Sound
1500 N Warner St
Tacoma, WA 98416

² Minerals and Geology Management
U.S. Forest Service
333 SW 1st Ave
Portland, OR 97204

⁶ U.S. Geological Survey
Box 25046, MS 974
Denver, CO 80225

INTRODUCTION

The Brinnon 7.5-minute quadrangle straddles Hood Canal and extends 5 mi west into the Olympic Mountains. Altitudes in the quadrangle reach 3500 ft along the Mount Jupiter trail (sec. 31, T26N R2W), and water depths 560 ft (secs. 27 and 28, T25N R2W) south of Black Point. (See Table A1 caption for explanation of altitude statements and sea level references.) Bedrock of the Eocene Crescent Formation (unit Ev_c) is mapped at the surface in one third of the quadrangle, where bedding and flow tops generally dip southeast to east. It is unconformably overlain by Quaternary sediment primarily deposited by glacial ice advancing from north of the map area (northern-sourced) and the Olympic Mountains (Olympic-sourced). This mostly glacial sediment generally forms a thin, discontinuous drape, commonly too thin or spotty to map, but dominant below 500 ft altitude. It likely reaches its maximum thickness east of Hood Canal, where Jones (1996) relied on well records and marine seismic reflection shots to suggest more than 300 ft but less than 600 ft of sediment. However, we agree with Daneš (1985) in suggesting about 1600 ft of sediment. We base our bedrock depth estimate on magnetic data (Richard Blakely, U.S. Geological Survey [USGS], written commun., 2011), gravity data (Blakely, written commun. to Trevor Contreras, 2010; Lamb and others, 2012), seismic line data (Lamb and others, 2012), magnetic survey data and interpretations (Lamb and others, 2012), and our interpretation of horizontal-vertical spectral ratio (HVSr) passive seismic data (Methods section; Table 1 on map plate) from significant site S1 (sec. 25, T25N R2W).

METHODS

We show as geologic units those deposits that we thought form a sufficiently thick surficial cover to be of geotechnical significance, generally 5 ft or more. Where stiff, impermeable, or geotechnically challenging units (for example, lodgment till or peat) were found or we sought to illustrate a geologic process, we locally mapped thinner deposits. In most areas, we relied partly on geomorphology, field relations, and, where available, well records, geotechnical studies, and prior mapping (Friskien, 1965; Carson, 1976; Garcia, 1996; Tabor and Cady, 1978; Grimstad and Carson, 1981; Yount and Gower, 1991). We used the Udden-Wentworth scale (table 5 in Pettijohn, 1957) to classify unconsolidated sediments. A U.S. Geological Survey (USGS) 7.5-minute topographic map was used as a base map, but contact locations other than shorelines were commonly refined by reference to field observations, lidar (light detection and ranging)(Puget Sound Lidar Consortium, 2000, <http://pugetsoundlidar.ess.washington.edu/index.html>), and aerial photos. We used the time scale of the USGS Geologic Names Committee (2010), and therefore made a distinction between post-glacial and Holocene. At HVSr stations (significant sites S1–S9; Table 1

on map plate), we used a formula from Kramer (1996; see also Lane and others, 2008) to infer depth to bedrock or another unit marked by a seismic velocity increase relative to overlying deposits:

$$\text{Depth} = V_s / (4 * (f_r))$$

where V_s is the mean shear-wave velocity in the deposits above the estimated depth, and f_r is the resonant frequency corresponding to peak HVSr. We assumed a mean V_s of 400 m/s (Bilderback and others, 2008). Our interpretation of lithologic descriptions and geotechnical data in well and boring logs near our surface HVSr sites confirms that the V_s value (400 m/s) is suitable for the sites. The f_r value we used for each station is shown in Table 1 as a number behind the HVSr station number (for example, S1, where f_r is 0.20). Thus, for station S1:

$$\text{Depth (m)} = 400 / (4 * 0.2) = 500 \text{ m, or } 1600 \text{ ft}$$

HVSr points in the cross section are plotted at the suggested geologic contact depths; their surface locations are shown on the map.

DISCUSSION AND ANALYSIS

Sediment Provenance and Lithology

Except for post-glacial alluvium and peat, which are minor outside the floors of the Duckabush and Dosewallips River valleys, sediment in the map area is mostly drift deposited as a result of Cordilleran ice sheet incursion into the map area during the Vashon Stade of the Fraser Glaciation. Earlier incursions of the Cordilleran ice sheet and alpine glaciers of the Olympic Mountains no doubt occurred, but their deposits are rarely exposed in the map area. Northern- and Olympic-sourced sediments resemble each other west of Hood Canal more than in most of the Puget Lowland because on its way into the map area, Cordilleran ice picked up material from the Olympics in addition to its load from the Canadian Coast Mountains, the San Juan Islands, and the northwestern Puget Lowland.

Sediment in the map area consists of (1) Olympic-provenance clast assemblages of basalt, sandstone, and their common accessories and weathering products (chlorite, calcite, monocrystalline and polycrystalline quartz, and zeolites), and (2) a mix of Olympic-provenance rocks and a broadly similar but more diverse northern-provenance assemblage. Diagnostically northern-provenance rocks include granitic and high-grade metamorphic rocks (Friskien, 1965). West of Hood Canal, mixing of Olympic- and northern-sourced sediments is such that we rarely estimated more than 1 percent diagnostically northern-provenance clasts, even in exposures of northern-sourced deposits (Fig. B1). Friskien (1965), like us, noted that northern-provenance clasts die out westward. The importance of local provenance (supplanting distal contributions) is illustrated by till at significant site S25, where lodgment till is draped on basalt bedrock of the upper Crescent Formation; grooves in the basalt indicate valley-parallel ice flow, thus requiring a distal ice source (Olympic or Cordilleran). Till clasts and matrix are 99 percent basaltic, consistent with an upper Crescent Formation provenance, and not representative of the source areas of either Dosewallips valley (Olympic) ice or Cordilleran ice (Table B1; Fig. B2). This indicates that distal ice accumulated the material for this till from nearby upper Crescent Formation substrate. (We interpreted the till as of Vashon age, deposited by the Puget lobe of the Cordilleran ice sheet moving west.)

The scarcity of diagnostically northern-provenance constituents in Brinnon-area drift suggests that Puget lobe-related ice rafting did not introduce much northern-provenance material into Olympic drainages. We therefore assume the presence of northern provenance clasts to be indicative of northern-sourced drift, and we assume that a lack of recognition of northern-provenance clasts, especially in small, muddy, or otherwise limited exposures, need not imply Olympic source. However, we (unlike Bretz, 1913) also noted rare granitic clasts within the Quatsap Point delta (unit Qpu), even though its location, scale, and orientation strongly suggest it was fed by the ancestral Duckabush River. (See additional discussion in unit Qpu description.)

We mapped some deposits that lack clasts of a diagnostically northern provenance as Vashon and associated with Cordilleran ice. Conversely, the provenance of deposits that we mapped as Olympic-sourced is debatable because it is defined on the basis of lithology. We know that this measure can be insufficient because both northern- and Olympic-sourced deposits can lack granitic and high-grade metamorphic clasts. Fluting, striations, or field relations allowed us to associate many Vashon deposits with a northern-sourced ice mass, but such pointers were not available for pre-Vashon deposits. We therefore assigned apparent provenance of some exposures partly from depositional location and the character of surrounding exposures. In addition, we used previous mappers'

interpretations as tie breakers, but in the end, the provenance we assigned for some deposits remains speculative. Thin-section petrography proved helpful in addressing this source versus provenance quandary.

Petrographic thin-section analysis documented that sediment derived from (1) upper Crescent Formation is heavily dominated by basalt, (2) mixed Crescent Formation and Olympic core rocks is marked by low basalt content coupled with moderate lithic fragment content, and (3) a northern source is marked by low to moderate basalt content and 0 to 15 percent plutonic and metamorphic lithic clasts and minerals, notably granitic rocks, high-grade metamorphic rocks (above prehnite-pumpellyite facies), and microveining within polycrystalline quartz. We deem this northern-source composition as diagnostic of provenance from the Coast Mountains of British Columbia, supplemented, we presume, by rocks from the San Juan Islands and the northwestern Puget Lowland (Table B1; Fig. B2). Our review of 94 thin sections suggests northern provenance for most drift deposits that lacked identifiable granitic clasts in hand sample, such as at significant site S27 (NE¼ sec. 25, T26N R3W).

We agree with Frisken (1965) in associating nearly all surficial drift in the map area with northern-sourced ice. Significant site S26 (sec. 18, T26N R2W) marks the westernmost longitude at which we noted granitic clasts in Rocky Brook valley. West of site S26, drift exposures thin, consistent with northern-sourced ice moving upvalley. At significant site S24 and west to the map edge, we favor Puget lobe residual ice instead of Olympic valley ice as the source of late Vashon ice-contact deposits because most of our thin-section analyses of drift deposits in the valley favor a northern sediment source. (A few samples are inconclusive, but only S25—discussed above—favors [a proximal] Olympic source.) Frisken's interpretation that no surficial Olympic drift is present within the Brinnon quadrangle, even though end moraines and till barely west of the map area represent Olympic ice advances, contributed to our decision to associate nearly all surficial drift in the map area with Puget lobe ice. However, Garcia (1996) argued that ice-contact deposits about 2.8 mi northwest of the Dosewallips River mouth (significant site S24) represent a late Vashon, Olympic-ice terminal moraine coeval with construction of the Brinnon delta (date site GD2 and nearby unit Qgol), and Bretz (1913) interpreted the till beneath the Brinnon delta and slightly north along the marine shore (secs. 34 and 35, T26N R2W, and sec. 3, T25N R2W) as Olympic-sourced.

We mapped all surficial drift north of the Brinnon delta as Vashon (Puget lobe) in part because, unlike Bretz, we found granitic clasts in some till exposures near the delta.

Except for post-glacial alluvium and mass-wasting deposits, we identified very few deposits as Olympic-sourced and found them sufficient for mapping only in the Fulton Creek basin (secs. 19 and 30, T25N R2W; sec. 25, T25N R3W; and Protraction Block [PB unsurveyed] 47, T25N R3W). All but one consisted of cobbles, pebbles, or diamicton. We interpreted these as drift (unit Qapd) in part because we reasoned that nonglacial times would be dominated by erosion, as is the case today, whereas voluminous valley trains and piedmont deposits of pebbles, cobbles, and diamicton would accumulate in response to Olympic ice advances, similar to the pattern found by Crandell (1964) and Thackray (2001) on the west side of the Olympic Mountains. Paleo-floodplain sediment at radiocarbon date site GD4 along Fulton Creek was mapped as unit Qpu_{op} (PB 47, T25N R3W) because we lacked strong reasons to classify it as either glacial or nonglacial. Other Olympic-sourced sediment that may or may not be associated with Olympic ice advances was included with Vashon advance sediment (unit Qga, otherwise associated with northern provenance) because its deposition resulted from damming of valleys by Puget lobe ice (for example, radiocarbon date site GD3).

Ice Limit

From our observations and prior work, we mapped the Vashon (Puget lobe) ice limit at about 3100 ft altitude, with a west-down slope. Like Frisken (1965), we show a 3100 ft ice limit around Mount Turner. Thorson (1980) cited a 1978 written communication from William Long (U.S. Forest Service) for a Vashon Puget lobe ice limit at 1006 m (3300 ft) at or near Mount Turner (see also Long, 1974, 1976). We observed till as high as 2660 ft north of Mount Turner (significant site S28) and at 3100 ft along Mount Jupiter Trail (significant site S29). We interpret the latter as northern-sourced because 500 ft south of S29 at significant site S30 (3030 ft) we found till with ample polycrystalline quartz that contained microveining, indicative of a northern source (Table B1; Fig. B2; Sediment Provenance and Lithology section). We see further support for a northern source in Long's (1974, p. 16) report of Vashon "granite erratics ... on the ridge extending eastward from Mount Jupiter to a maximum altitude of 2900 feet." We recognize that a prior northern ice mass extended slightly farther south than Vashon ice and therefore may have been slightly thicker, but we interpret the till at significant sites S29 and S30 as Vashon age because (1) Long interpreted his granite erratics as Vashon, (2) the slight till weathering we observed is consistent with the partially inherited weathering characteristics of Vashon Till we commonly observed elsewhere in the map area (see section on

weathering of till), and (3) Thorson's (1980) regional modeling of the thickness and extent of the Vashon Puget lobe ice suggests an ice limit between 1006 m (3300 ft) at or near Mount Turner and 762 m (2500 ft) south of the Duckabush River.

Like Frisken (1965), we show a westward drop in ice-limit altitude because we saw no till above 1900 ft along the western map edge. This favors association with northern-sourced ice because Olympic ice would have sloped east-down. However, the westward gradient is poorly constrained. Puget lobe ice incursions into Olympic Mountains valleys would have met Olympic ice or (and?) impounded lakes, potentially resulting in an unstable and uneven ice margin. Moreover, the assumption that the reference points for the following ice-limit estimates are of coeval origin is debatable. In Fulton Creek valley near the southern map edge, Long (1976) noted a westward drop of 500 ft/mi. In Rocky Brook valley, about 3.5 mi separates the 3100 ft ice limit at Mount Turner from the apparent western limit of Vashon Puget lobe ice at about 2100 ft, slightly west of the map edge (Long, 1975), for a westward slope of about 300 ft/mi. A roughly 3.2 mi distance between our uppermost observed till exposure at 3100 ft (significant site S29) and Frisken's (1965) western ice limit 1.5 mi west of the map edge in the Duckabush and Dosewallips valleys suggests a slope of nearly 900 ft/mi. The ice limit lines shown on our map are at best approximate and assume validity of the above estimates.

Differentiation of Till Deposits

WEATHERING OF TILL

We identified few exposures of pre-Vashon sediment in the map area. Frisken (1965, p. 29) noted that "from the Hamma Hamma [River] to the northern edge of the Brinnon quadrangle all the Puget drift exposed seems to be of Vashon age", and that there "is little apparent difference in the composition or weathering ... of the drift ... at any altitude along the front of the Olympic Mountains ... [and nowhere in] the Brinnon quadrangle could Vashon drift be shown to overlie older drift." He also argued that drift higher than about 1950 ft is pre-Vashon. In light of our interpretation that the Vashon ice limit approximates the uppermost drift exposures in the map area (see Ice Limit section), we assumed that unless we have specific reason to assign a surficial northern-sourced till to an older ice advance, it is probably a Vashon deposit. Like Todd (1939), Bretz (1913), Frisken (1965), and Long (1974), we found that we could not systematically relate degree of weathering to depositional age in this map area, although other workers did so southwest of the Brinnon quadrangle (Carson, 1980; Contreras and others, 2012a,c). We mapped some exposures dominated by weathered clasts and matrix as Vashon drift because the weathering may be mostly inherited from locally derived, already-weathered pre-Vashon sediment and bedrock, a mechanism also envisioned by Carson (1980) and Polenz and others (2012a,b). We arrived at this interpretation particularly where weathering in clasts and matrix proved bimodal: fresh (unweathered) clasts and matrix among much more severely weathered (commonly rotten) particles, with no apparent systematic relation of weathering severity to particle mineralogy. Moreover, had we systematically attributed moderate or advanced weathering of surficial deposits to pre-Vashon deposition, there would have been very little Vashon-age drift to map. We rejected that approach on the basis of our impression that some exposures within the same drift displayed considerable lateral weathering variation and on the assumption that the most recent large ice mass is also the most likely to dominate surficial deposition, especially because drift (and especially till) in the map area is typically thin and discontinuous and commonly rests directly on bedrock. Our bias toward associating surficial deposits with Vashon ice may have resulted in some errors, but we suspect that they are fewer than if we were to assign more surficial deposits to prior ice advances on the basis of at least partially inherited weathering.

The apparent ability of workers in the Hamma Hamma basin (Carson, 1980; Contreras and others, 2012a) to separate drifts by degree of weathering, in contrast to the inability of other workers in the Brinnon area (Frisken, 1965; Long, 1974; this study) to do the same, may point to divergent patterns of glaciation, drift deposition, and weathering. The Brinnon quadrangle is dominated by bedrock slopes that have discontinuous and mostly thin sediment cover. Steep ridges separate the Duckabush and Dosewallips drainages within the quadrangle, and one would expect that major valley glaciers would originate at least 10 mi west of Hood Canal. Drift is concentrated close to Hood Canal and within the Dosewallips and Duckabush valleys. In contrast, drift-covered foothills of the Hamma Hamma watershed extend 2 to 3 mi inland, and the entire watershed rests within 12 mi of Hood Canal. Olympic glaciers in the Brinnon quadrangle have farther to travel before reaching Hood Canal than do Olympic glaciers south of the map area, where broader foothills may also better accommodate deposition and preservation of drift of both northern and Olympic provenance.

Hellwig (2010) and unpublished precipitation data show a marked northward decrease in historical precipitation: Wash. State Dept. of Natural Resources (DNR) data show 60 to 130 in. of mean annual rainfall in the Hamma Hamma watershed versus 45 to 75 in. in the Brinnon area (103-year western Washington composite record, DNR intranet, 2012). Mark Bruskiewicz (Wash. State Dept. of Transportation [WSDOT], written commun., 2012) stated that WSDOT supplied the data to DNR and obtained it in 2006 from the PRISM Climate Group at Oregon State University (http://www.prism.oregonstate.edu/docs/meta/ppt_103yr.htm). If Pleistocene precipitation patterns included a comparable differential, one would expect more Olympic ice in the Hamma Hamma watershed. Indeed, Frisken (1965, p. 49) noted that “the Hamma Hamma Valley appears to have been more extensively glaciated than” the other major drainages of the eastern Olympic Mountains. Carson (1980) speculated on a link between precipitation and the lack of Olympic till in the lower Duckabush and Dosewallips valleys. Less precipitation in the Brinnon quadrangle would also likely result in less weathering, and workers there would be less likely to be able to separate drifts by small differences in weathering. Finally, it may matter that sedimentary interbeds among basalt flows are rare and thin in the Brinnon quadrangle, as are pillow basalts. Both are more common in the Hamma Hamma watershed, and the subaqueous basalt deposition required by pillow formation may also have set the stage for more efficient bedrock weathering there. The Fulton Creek watershed at the southwest end of the Brinnon quadrangle may be a transition zone on all above accounts.

AGE OF TILL

Unless our above observations and interpretations regarding till weathering are misguided, exposures of pre-Vashon till are rare in the Brinnon quadrangle. The few exceptions (see units Qpd and Qapd) are undated but tend to be more uniformly weathered than Vashon Till. A new $14,490 \pm 60$ yr BP radiocarbon date from Rocky Brook valley (2σ age range between 17.8 and 17.5 ka; date site GD3; Table A1) constrains the arrival of Vashon ice at 1350 ft altitude between the sample site and the mouth of the Dosewallips valley (see also unit Qga). The constraint on the advance of the Puget lobe is approximate because the sample site is 4 mi northwest of the mouth of the Dosewallips valley, and it is unknown how much time passed from the time that ice first reached the latitude of Dosewallips valley until the ice thickened enough to invade the mountains and impound the lake that trapped the sample we dated. The possibility of in-built age in radiocarbon samples (Gavin, 2001) additionally suggests that sample deposition could be as much as 600 years more recent than the time of wood growth represented by the date, potentially cancelling out the time lag mentioned in the previous sentence. Hence we can say only that Vashon ice entered the map area roughly 18.5? ka (17.8 ka plus some unknown amount of time to thicken enough to reach the date sample site) to 17 ka (17.5 ka less 600 yr to allow for a possible inbuilt age plus 100 yr to allow the ice to thicken enough to reach the sample site). Radiocarbon dates at three sites in the Hoodsport and Union quadrangles between 20 and 33 mi south of date site GD3 (Polenz and others, 2010a,b; 2012a,b) indicated a Vashon ice arrival time there between about 17 and 15.3 ka. This suggests that Puget lobe ice took between 0 and perhaps more than 3500 yr to advance from Brinnon 20 to 33 mi to the south. These estimates are consistent with prior speculations (Logan and Walsh, 2009; Polenz and others, 2012b) that the Vashon ice sheet advanced across the Puget Lowland later than envisioned by Porter and Swanson (1998) and Booth and others (2004), then stalled at its southern terminus and quickly began to disintegrate (Logan and Walsh, 2009; Haugerud, 2009; Polenz and others, 2012b), although patches may have persisted for millennia (Porter and Carson, 1971).

Ice-dammed Vashon Recessional Lakes

Midslope benches that can be seen in lidar-based images suggest relict shorelines between altitudes of about 315 ft (at the southern map edge, “Upper Fulton Creek delta” of Thorson, 1981) and about 380 ft (outwash terrace above Spencer Creek, northeastern map corner). None of our field observations provided clear evidence for such shorelines, and in some areas on the north sides of both the Dosewallips and Duckabush valleys, multiple bench altitudes between about 315 and 350 ft are associated with ice-contact deposits (units Qgic and Qgik). However, a plot of bench altitudes from six points spread south to north across the map area above the west shore of Hood Canal (Table C1; Figs. C1, C2) suggests a single shoreline that is rotated south-down roughly to the extent suggested by Thorson’s (1989) regional rebound tilt analysis. Our shoreline coincides in altitude with a shoreline Thorson (1981) identified south of the Duckabush River, which he assigned to glacial Lake Hood. Bretz (1913) suggested a 220-ft lake shore altitude for glacial Lake Hood at the Brinnon delta, where we noted no shoreline at that level. We did see an apparent shoreline above the Brinnon delta at about 357 ft altitude. A best-fit line through our bench data points would reach the south end of Hood Canal at Purdy Canyon (25 mi southwest of the map area) at 154 ft (Fig. C2);

this is significantly below the 240-ft altitude of the lowermost outwash channel that Polenz and others (2010a, p. 15) recognized and identified as a possible spillway from a lake in Hood Canal to glacial Lake Russell at Oakland Bay (27 mi south of the map area). Possible reasons for a similar discrepancy associated with shorelines farther south along Hood Canal in the Hoodsport and Skokomish Valley quadrangles were presented by Polenz and others (2012b) and include an unrecognized, lower lake drain and tectonic or isostatic land level changes. They appear to apply similarly here. Postulated shoreline fragments north and south of the Brinnon delta (at 135 ft), and apparently belonging to the same glacial lake, follow a comparable south-down trend, descending to about 95 ft at the southern map edge and the “Lower Fulton Creek delta” of Thorson (1981, p. 40, 50) 0.5 mi south of the map area. They include prominent flats at about 100 ft north and south of the mouth of the Duckabush River, where lake sediments underlie at least some of the flat surfaces. Apparently correlative outwash and kame terraces can be traced for at least 2 mi west into the Duckabush valley, rising to 160 ft (Fig. C3).

STRUCTURE

The Brinnon quadrangle is in the Cascadia subduction zone forearc, where active structures accommodate margin-parallel shortening due to oblique convergence at the subduction zone (Johnson and others, 2004). Crustal earthquakes in and near the map area (Fig. D1) show that it is seismically active.

Faults and joints in seemingly random orientations abound in Crescent Formation basalt. Few are associated with appreciable gouge or surface expression, and nowhere did we document post-glacial offset. Systematic structural analysis would require statistical evaluation of more structural measurements than we were able to collect and process. We thus show joints and shears in the Crescent Formation where outcrops reveal a particularly well developed joint set, a clearly dominant joint orientation, or shears accompanied by well-developed slickensides and (or) gouge more than 1 ft thick.

In the north half of the map, we found no systematic trends, very few notable fault exposures, and no structures that we could trace across more than one exposure. The regionally prevalent east- to southeast-dipping Crescent Formation flow orientation was not clearly evident (see also Yount and Gower, 1991). This suggests undocumented structural complexity, particularly in the west half of the map area north of the Dosewallips River, where a sub-vertical, northwest-trending fault with 2-ft-thick gouge (1 mi northwest of date site GD7) is the most impressive fault we saw anywhere in the map area (Fig. D2). The boundary between the upper and lower members of the Crescent Formation has been mapped 0.2 mi west of the fault at scales smaller than 1:24,000, as have clusters of mostly north-trending folds within 3 mi northwest and southwest of the exposure (Tabor and Cady, 1978; Gerstel and Lingley, 2003).

Topographic features (ridges, valleys) and some strong magnetic anomalies (magnetic data courtesy of Richard Blakely, USGS, written commun., 2011) south of the Dosewallips valley are preferentially aligned west to slightly northwest, and joint orientations clearly control the west- to west-northwest alignment of some stream reaches, as at significant site S33 (Fig. D3). We were unable to document faulting associated with these joints but note that they parallel and thereby suggest possible westward extension of proposed folds and fault strands (map plate; Lamb and others, 2012) associated with the active Seattle fault, extensively studied east of Hood Canal (for example, Raisz, 1945; Daneš and others, 1965; Rogers, 1970; Bucknam and others, 1992; Atwater, 1999; Brocher and others, 2001; Blakely and others, 2002; Nelson and others, 2002, 2003a,b,c; Martin and others, 2007; Karel and Liberty, 2008; Kelsey and others, 2008; Liberty and Pratt, 2008; Pratt and Troost, 2009; Tabor and others, 2011; Mace and Keranen, 2012). Related faulting has been inferred across Hood Canal (Anderson and others, 2008; Lamb and others, 2009a,b) and into the map area from magnetic, gravity, and seismic data (Andrew Lamb, Boise State Univ., written commun., 2012; Lamb and others, 2012). Bedrock is exposed along the west shore of Hood Canal south of Lamb and others' (2012) northernmost proposed fault strand, but not within 2000 ft north of that fault strand, consistent with the proposed offset. Our flow orientation measurements along the shore are consistent with the presence, location, and character of our proposed faults and folds, which we adopted from Lamb and others (2012). On the basis of available offshore seismic profiles and onshore flow and bedding orientations, we are more confident in our interpretation of folds than of faults, and that is reflected in the coding of the structures where they come ashore. We also modified the southernmost of Lamb and others' (2012) three postulated fault strands in the map area by aligning segments with faint lineaments we saw in the lidar data. A small stream across one segment reveals bedrock upslope but not downslope of the scarp, consistent with the south-up offset suggested by Lamb and others (2012), although the lineament itself appears partly marked by north-up topography. A pool of water in the channel (otherwise dry) suggests a possible spring at the postulated fault.

A cluster of roughly west-trending joints that resemble those noted above, and associated faults, were identified by Contreras and others (2012a) southwest of the map area. All of these faults and joints may be part of a convergence of the west-trending Seattle fault and the northeast-trending Saddle Mountain fault zone, which is also post-glacially active (Carson, 1973; Wilson, 1975; Wilson and others, 1979; Hughes, 2005; Witter and Givler, 2005; Witter and others, 2008; Blakely and others, 2009; Czajkowski and others, 2009; Polenz and others, 2012a,b).

We show a queried “lineament and alignment of geomagnetic anomalies and crustal earthquakes” from the southwest corner of the map trending northeast to the eastern map edge. The lineament was first noted when contemplating a lidar composite image of blended vertical and northeastern illuminations, and it crudely follows topographic troughs, Pleasant Harbor being the most distinctive. It aligns with a geomagnetic gradient northeast of Pleasant Harbor and three crustal earthquake epicenters within 2 mi east of the eastern map edge (Fig. D1) and one 4 mi southwest of the western map edge. Contreras and others (2012a) show a southwesterly extension of the lineament into the Eldon 7.5-minute quadrangle and recognized shearing along part of the lineament. In the Brinnon quadrangle, the lineament marks the approximate western limit of at least the northern two of Lamb and others’ (2012) three postulated Seattle fault strands, suggesting that it may itself be structural. The termination of these fault strands in this area is also supported by an apparent lack of westward continuity of the geomagnetic anomalies that partly support mapping these structures to the east. If the lineament is a tectonic structure, it may explain why two large landslides in the Duckabush valley (one dated as active about 1.26 to 1.3 ka, date site GD8, Table A1) are conspicuously close to the lineament and why the spacing between parallel, west-dipping shears (Bretz, 1913) (and fewer, possibly conjugate, east-dipping ones) in the Quatsap Point delta decreases toward the west end of the exposure. The shears show normal apparent offset of as much as 1 ft each and were interpreted by Bretz (1913) as faulting due to uplift. They do not penetrate upsection Vashon drift, and their westward clustering would seem unlikely to result from glacial loading (because we would expect such loading to be more uniform).

Daneš and others (1965) inferred a northeast-trending Hood Canal fault from gravity and magnetic data. It was mapped beneath Hood Canal from high-resolution seismic data (Haug, 1998) and tomographic modeling (Brocher and others, 2001). The fault may cross the southeast corner of the Brinnon quadrangle and may be represented by messy seismic reflection within a mile of the southern map boundary (see between structures F2 and A3 in fig. 5C of Lamb and others, 2012). However, like Lamb and others (2009a, 2012), we do not show this fault because magnetic data fail to reveal an associated anomaly. The faults we do show suffice to account for the evidence we see for tectonic deformation.

We did not find strong evidence of post-glacial tectonic deformation (other than glacial-isostatic rebound tilt) within the map area. However, one way to interpret the elevation and tilt of apparent relict lake shores above Hood Canal is that since the end of the Vashon Stade (the east half of?) the map area has been lowered relative to the south end of Hood Canal (Table C1; Fig. C2; see also Ice-dammed Vashon Recessional Lakes section). If so, post-glacial tectonic deformation along Hood Canal may have been greater south of the map area than within it, consistent with greater scatter in relict shore levels noted by Polenz and others (2012b) south of the map area (see also Table C1; Fig. C2).

DESCRIPTION OF MAP UNITS

Quaternary Unconsolidated Deposits

HOLOCENE NONGLACIAL DEPOSITS

- af **Artificial fill**—Sand, cobbles, pebbles, boulders, silt, clay, organic matter, rip-rap, and concrete placed to elevate the land; engineered or non-engineered; shown where readily verifiable, fairly extensive, and apparently thick enough (>5 ft) to be geotechnically significant; excludes roads.
- ml **Modified land**—Locally derived sand, pebbles, cobbles, boulders, silt, clay, and diamicton excavated and redistributed to modify topography; underlying units exposed in some cuts; locally includes concrete and artificial fill; shown where fairly extensive and apparently thick enough (>5 ft) to be geotechnically significant; excludes roads and inactive pits where underlying units can be identified.
- Qb **Beach deposits**—Sand, pebbles, pebbly sand, cobbles, silt, clay, shells, and isolated boulders; loose; clasts typically moderately to well rounded and oblate; locally well sorted; derived from shore bluffs,

streams, and underlying deposits. Unit Qb is transient in the modern environment; erosion at times exposes underlying units. The age of unit Qb is constrained to less than about 6000 yr because before that time, sea level was much lower (Dragovich and others, 1994; Mosher and Hewitt, 2004).

Qa_m, Qoa_m **Marine deltaic alluvium**—Sand, mud, and, especially in channel bedload facies, pebbles and cobbles; includes some organic salt-marsh deposits; clasts and matrix generally fresh; loose; clasts typically well rounded; moderately to well sorted; stratified to massively bedded; deposited in tidally influenced, deltaic distributary channels and tidal flats; distinguished from unit Qa by presence of brackish water. Like unit Qb, the age of unit Qa_m is constrained to less than about 6000 yr. Subunit Qoa_m (cross section only) resembles unit Qa_m but is older and forms relict deposits. Organic-rich mud from the Duckabush delta yielded a radiocarbon age estimate of 1350 ±90 yr BP (Table A1, sec. 22, T25N R2W) and was assigned to unit Qoa_m because it was buried, suggesting a relict deposit no longer likely to be reworked as part of unit Qa_m. This does not imply that unit Qa_m is everywhere younger than about 1350 yr BP.

HOLOCENE TO POST-GLACIAL PLEISTOCENE NONGLACIAL DEPOSITS

- Qp **Peat**—Organic and organic-rich sediment; includes peat, gyttja, muck, silt, and clay; typically in closed depressions; commonly mapped on the basis of topography or aerial photos; mapped in all recognized wetland areas and flat-bottomed closed depressions unless a different unit or standing water was identified.
- Qls **Landslide deposits**—Cobbles, pebbles, sand, silt, clay, boulders, and diamicton in landslide bodies and toes; angular to rounded clasts and grains; unsorted; generally loose, jumbled, and unstratified, but locally retaining primary bedding and compaction; commonly includes liquefaction features. Absence of a mapped slide does not imply absence of sliding or hazard. Many slide areas are unmapped because steep slopes, beach waves, or active streams have dispersed slide deposits. Slides not recognized with confidence are shown as unit Qmw. Some slide areas include exposures of underlying units. Where map scale permits, head scarps are identified by a scarp symbol. Where Contreras and others (2012a) mapped unit Qls in the head scarp of a landslide along Fulton Creek (sec. 30, T25N R2W), the exposed geologic units are identified in the Brinnon quadrangle, resulting in a map-edge mismatch.
- Qmw **Mass-wasting deposits**—Cobbles, pebbles, sand, silt, clay, boulders, and diamicton; typically loose; generally unsorted; locally stratified; mapped along mostly colluvium-covered or densely vegetated slopes that are potentially or demonstrably unstable; locally includes alluvial fans, debris fans, landslides too small to show separately or that could not be confidently mapped, or exposures of underlying units. Where fan shaped, unit Qmw generally covers steeper slopes than unit Qaf. Absence of a mapped mass-wasting deposit does not imply absence of slope instability or hazard.
- Qa, Qoa **Alluvium**—Boulder, cobble, and pebble gravel and sand, with some silt, clay, and peat; clasts and matrix generally gray and fresh, but some exposures iron-stained; loose; clasts typically well rounded and moderately to well sorted; stratified to massively bedded; deposited in streams and on flood plains and terraces. Shear-wave velocity profiles south of the map area indicate that unit Qa in some locations is texturally more diverse than unit Qgic (Polenz and others, 2009a). The unit may locally include some recessional outwash (unit Qgo). Subunit Qoa resembles unit Qa but is older and forms elevated relict terraces that (unlike terraces mapped as unit Qgo) lack evidence to link them to a recessional glacial environment. However, unit Qoa likely includes some recessional glacial deposits. The relict character of unit Qoa is documented by a radiocarbon date of 4140 ±30 yr BP at site GD1 (Table A1) in the lower Dosewallips valley, where we interpreted a concentration of charcoal in unit Qoa as part of a post-fire sediment pulse. We doubt that such a pulse alone would have triggered enough aggradation to form this terrace, which is now 15 to 20 ft above the active flood plain; we suspect a downvalley logjam or landslide channel blockage at or near significant site S34 (2500 ft southeast). Garcia (1996) reported a 3570 ±60 yr BP radiocarbon date on charcoal from relict stream terraces west of the Brinnon quadrangle (his map unit Het). Although the stated age ranges of the two radiocarbon dates do not overlap, the terraces may represent the same sediment pulse, and the ages may be equivalent because charcoal dates

can contain in-built age (Gavin, 2001). Alternatively, tectonic tilting could explain aggradation and later re-excavation of the valley floor. Although the region is tectonically active (see Structure section), we have identified neither a tectonic mechanism nor other evidence for such tilting. Along stream reaches graded to modern sea level, units **Qa** and **Qoa** should be younger than about 6000 yr (see unit **Qb**). The distribution of units **Qa**, **Qoa**, **Qam**, and **Qoam** in the cross section is supported by analysis of geotechnical and well-drilling reports (Shannon & Wilson, Inc., 1998) and seismic records, which suggests that modern storm events may locally scour channels to a depth of 20 to 30 ft. It also suggests that the Dosewallips River main channel near its delta may have aggraded with little lateral migration and may have at times avulsed to a more northerly alignment. Multiple generations of apparent channel scour depth profiles and postulated relict channel positions are illustrated by “armored channel bases” in cross section A'-A”.

Qaf, Alluvial fan deposits—Cobble and pebble gravel with sand, silt, and boulders; loose; moderately to poorly sorted; stratified to poorly stratified; forms concentric lobes where streams emerge from confining valleys. Deposition is commonly sudden, hazardous, and associated with significant storm events, such as the storm of December 1 to 3, 2007 (Sarikhani and others, 2008). Relict fan deposits that have stopped accumulating are identified as subunit **Qoaf**; their surface is typically dissected by a modern stream channel that is deep and steep enough to pre-empt addition of modern sediment. Unit **Qgoaf** is distinguished from unit **Qoaf** because field relations suggest or require deposition of unit **Qgoaf** coeval with Vashon recessional outwash. For example, the large, dissected, relict fan segments at the base of Marple and Spencer Creeks (secs. 13 and 14, T26N R2W) were assigned to unit **Qoaf** because the modern creeks are too incised to add to the fan.

PLEISTOCENE GLACIAL AND NONGLACIAL DEPOSITS

Vashon Drift (northern-sourced)

Qgo Vashon recessional outwash—Pebble gravel, in many exposures cobbly, with some sand interbeds and mostly clean sandy matrix (<5% silt or clay), but commonly containing some silt and clay; clasts and matrix mostly fresh, but commonly iron-stained to brown, red, and yellow, and in some exposures more weathered than recent alluvium; loose, typically cohesionless but in places difficult to distinguish from the generally more compact unit **Qga**; clast rounding and sorting diverse, clasts most commonly subrounded and moderately sorted; typically stratified; typically 5 to 15 ft thick, 100 ft maximum observed thickness at the southern map boundary east of Fulton Creek. Unit **Qgo** was deposited by Vashon meltwater in outwash channels, depressions, or lakes. It typically covers perched terraces along valleys, where it tends to be more elevated than unit **Qoa**, and field relations suggest a recessional-glacial association. Deposits are commonly ice-proximal; some boundaries grade to unit **Qgic**. The unit overlies till and post-dates Vashon ice. Along the southern quadrangle boundary, a mismatch has resulted where granitic clasts indicated association with a northern source in the Brinnon quadrangle, whereas Contreras and others (2012a) mapped Olympic outwash to the south. Locally divided into:

Qgoaf Vashon recessional alluvial fan deposits—Cobble and pebble gravel, sand, silt, and boulders; loose; moderately to poorly sorted; stratified; forms concentric lobes where outwash streams once emerged from confining valleys. The relict fans no longer receive sediment and resemble those of unit **Qoaf**, but field relations suggest or show that the unit is Vashon recessional. The apparent depositional agent was meltwater. The unit was primarily recognized where lidar reveals dissected, relict fan morphology, suggesting that similar deposits went unrecognized where lidar was not available.

Qgol Vashon recessional glacial lake–deltaic outwash—Pebble and cobble gravel, sand, and local mud; generally brownish-gray; loose; moderately to well sorted and clean; at least 140 ft thick at Bretz’s (1913) “Brinnon Delta” (secs. 34 and 35, T26N R2W, and sec. 3, T25N R2W; cross section), the only place in the map area where it was identified; glaciofluvially deposited marginal to an ice-dammed lake, as a deltaic assemblage of pebbly to cobbly fluvial topset beds, pebbly, cobbly, or sandy deltaic foreset beds, and sand-dominated quiet-water lake-

bottom (bottomset) beds. Post-glacial entrenchment of the Dosewallips River in a narrow bedrock gorge may have prevented its erosion (Friskien, 1965). Our two new age estimates from the delta (date site GD2; Table A1)— 21.7 ± 2.50 ka by optically stimulated luminescence (OSL) and 36.7 ± 4.14 ka by infrared-stimulated luminescence (IRSL)—are older than regional radiocarbon data would suggest (~ 16 ka, Table A2). We suspect that partial bleaching (incomplete pre-depositional re-setting of luminescence signal) inflated our age estimates, as is common in glacial deposits (Rhodes, 2011).

- Qgof Vashon recessional(?) glacial lake deposits**—Silt, sand, clay, and rare dropstones; gray; loose, locally moderately stiff; clean. Well records suggest a thickness of 40 ft near the mouth of the Duckabush River. The only other mapped deposits are near the western map edge, where dropstones are concentrated in the basal 2 ft of 24-ft-thick exposures along the Dosewallips River channel margin.
- Qgic Vashon ice-contact deposits**—Cobble and pebble gravel, sand, discontinuous deposits of ablation, flow, and lodgment till, lacustrine mud, and isolated boulders; tan to brown or gray; loose to compact; poorly to well sorted; massive to well stratified; locally includes oversteepened beds that developed (1) due to sub-ice flow dynamics, (2) as collapse features following melting of nearby ice, or (3) by glacio(?) tectonic deformation; ranges in thickness from a few to at least 120 ft; primarily deposited late in the glaciation by meltwater and ice. This unit commonly includes stagnant-ice features (kettles, hummocky topography, ripples on flutes, disrupted surfaces on and between flutes, and subglacial or subaerial outwash channels). Where morphologic evidence for stagnant ice is weak or absent, unit Qgic is mapped from observation of poor development or absence of lodgment till, typically having less matrix mud than well-developed lodgment till (unit Qgt). Where stagnant-ice features are found, lodgment till is commonly absent or only a few feet thick, locally ranges to “sub-glacially reworked till” (Laprade, 2003), and tends to be more permeable than well-developed lodgment till. See also Polenz and others (2009a, 2010a) and Contreras and others (2012b) for discussion of the Fraser Glaciation, leaky till, and similarities among units Qgic, Qgo, and subunits Qgos, Qgof, and Qgol east and south of the map area. Some boundaries to unit Qgo are gradational. A map-edge mismatch with the Holly quadrangle has resulted where Contreras and others (2012c) inferred pre-Fraser deposits south of Fulton Creek. Where Contreras and others mapped Vashon recessional outwash east of Hood Canal, exposure of till and absence of terrace morphology support identification as unit Qgic. Locally divided into:
- Qgik Vashon ice-contact kames and kame deltas**—Pebble and cobble gravel, sand, lacustrine mud, and scattered lenses of diamicton; mostly loose but ranging to compact; medium- to very thickly bedded or massive; moderately to well stratified; locally contains delta foreset beds, crossbedding, cut-and-fill structures, and oversteepened or slumped bedding. These relict glaciofluvial-deltaic deposits were mapped where sedimentary structures, geomorphology, and (or) geologic setting provide evidence for ice buttressing of meltwater streams and lakes along hillslopes in the Dosewallips, Duckabush, and Fulton Creek valleys—primarily where lidar was available (southeastern two-thirds of the map area), suggesting that similar features may be present farther west and along Rocky Brook (secs. 17, 18, 20, 21, and 28, T26N R2W, and sec. PB38, T26N R3W), most likely where we mapped units Qgic or Qgo.
- Qgt Vashon Till**—Diamicton, mostly lodgment till, consisting of clay, silt, sand, pebbles, cobbles, and isolated boulders, typically supported by a sandy matrix; brown to gray, ranging to tan, red, and orange; typically lightly weathered or unweathered but locally includes rotten clasts and (or) matrix apparently incorporated from nearby weathered substrate; compact, with well-developed facies resembling concrete, but near the surface commonly hackly or looser and with loose ablation till composing the top 1 to 10 ft; clasts commonly striated and faceted, with subangular or rounded edges; unsorted; unstratified (but locally banded); forms a patchy and seemingly randomly distributed cover, with typical exposures 5 to 10 ft thick. The thickest clearly observed exposure is 30 ft thick, but in a poorly exposed sea cliff north of the Dosewallips valley, this unit appears to be about 60 ft thick. Unit Qgt was deposited directly by glacial ice. Basaltic, plutonic, and metamorphic erratics are common in and on till. Some exposures

include locally sheared and jointed layers or lenses of sand, pebbles, and cobbles. Unit **Qgt** typically dominates, but is discontinuous on, fluted surfaces and forms a thin, patchy draping over bedrock such that, especially at higher altitudes, many till contacts are poorly constrained. Fluting and striations are faint or absent in most of the map area. Unit **Qgt** is typically in sharp, unconformable contact with underlying units, most commonly bedrock or advance outwash (units **Ev_c** and **Qga**). Unit **Qgt** lies stratigraphically below unit **Qgo**. Well-developed lodgment till locally forms an effective aquitard, but varied till thickness and gradational association with more permeable ice-contact deposits and outwash channels suggest that the aquitard is leaky (Polenz and others, 2009a, 2010a; Contreras and others, 2012b; Haugerud, 2005). Unit **Qgt** may include unrecognized exposures of older till or Olympic-sourced till (unit **Qad**) (see Sediment Provenance and Lithology section). Obvious candidates for older till are weathered to rotten, red and orange to brown exposures that thinly drape weathered basaltic bedrock or soil at higher altitudes (where till commonly is too thin or spotty to map). Some prior workers (Friskén, 1965; Bretz, 1913; Carson, 1976, 1980) interpreted many such exposures as pre-Fraser till. We prefer to interpret most as Vashon Till because they include unweathered clasts and till matrix fragments among the weathered clasts and matrix. A map-edge mismatch has resulted where Contreras and others (2012c) mapped undivided pre-Fraser deposits (unit **Qguc₂**) west of Fulton Creek; exposures of lightly weathered surficial lodgment till with granitic clasts support our mapping of Vashon Till. Where Contreras and others mapped unit **Qls** in the head scarp of a landslide along Fulton Creek, the exposed unit **Qgt** in the Brinnon quadrangle results in a boundary mismatch.

Qga **Vashon advance outwash**—Pebble and cobble gravel, silt, sand, clay, and diamicton (typically apparent debris-flow deposits into glacial lakes); clean except in ice-proximal and glaciolacustrine deposits; gray to tan; generally compact (see fig. 4 of Polenz and others, 2009a), but commonly cohesionless; clasts typically well rounded and well sorted; very thinly to very thickly bedded, with planar and graded beds, cut-and-fill structures, trough and ripple crossbeds, and foresets, but ranges to structureless. At the southeastern map corner (Kitsap Peninsula) the unit is at least 230 ft thick. Well records show that the unit thickness exceeds 160 ft below the Brinnon delta (see cross section), where well W18 notes interbedded “sand”, “gravel”, “clay”, and “shale”, and it appears to exceed 100 ft in some banks along the lower Duckabush and Dosewallips valleys, along portions of Rocky Brook, and north of South Fork Fulton Creek. Unit **Qga** is typically of northern or mixed Olympic and northern provenance (generally containing <1% diagnostically northern-provenance clasts; Fig. B1) but includes lacustrine, Olympic-sourced valley fill deposited due to damming by Puget lobe ice, such as at radiocarbon date site GD3 along Rocky Brook north of the Dosewallips River. Unit **Qga** was deposited as proglacial fluvial, deltaic, and lacustrine sediment during the Vashon glacial advance and is typically overlain by units **Qgt** or **Qgic** along a sharp, unconformable contact. East of Hood Canal, sandy pebble and cobble gravel were the only observed facies. Exposures in Olympic Mountains valleys are mostly lacustrine. In smaller valleys, pebble or cobble gravel that has a muddy matrix dominates most lake deposits; in the Dosewallips and Duckabush valleys, mud or sand dominates. For instance, at significant site S23 in the lower Dosewallips valley (approximately located after Friskén, 1965) at least 50 ft of lacustrine section is largely free of pebbles and cobbles, suggesting a larger lake. Similarly, at least 25 ft of a well-laminated lacustrine facies was observed south of the Duckabush River (significant site S22), suggesting that in both the Duckabush and Dosewallips valleys, at least early in the Vashon Stade, ice of the Puget lobe impounded a lake rather than join Olympic valley ice (contrary to assertions of Bretz, 1913, and speculations of Friskén, 1965). Debris slides and debris flows due to wet storms (for instance, Sarikhan and others, 2008) are commonly dominated by pebbles and cobbles from unit **Qga**, confirming that the saturated unit is prone to rapid landslides. Well records east of Hood Canal and springs at the base of the fluvial gravel facies west of Hood Canal indicate that the unit is a major aquifer. This aquifer is sensitive to contamination because the upland surface, mapped as units **Qgt** and (or) **Qgic**, is commonly a leaky aquitard (Polenz and others, 2009a, 2010a; Contreras and others, 2012b; Haugerud, 2005). Unit **Qga** was generally identified by its stratigraphic position beneath Vashon Till, the presence of northern-provenance clasts or matrix, and its fresh appearance. Except at date site GD3, deposits within the unit are undated and probably include some pre-Vashon drift. At date site GD3, a 14,490 ±60 yr BP radiocarbon date on small, detrital wood fragments from lacustrine mud of Rocky Brook valley provenance suggests deposition between 17.8 and

17.5 ka (Table A1) and thereby identifies the time of Vashon ice arrival (see Age of Till section). Locally divided into:

- Qgas Vashon advance outwash sand**—Sand and local interbeds of silt, clay, pebbles, cobbles, or diamicton; generally clean; gray to brown; generally compact; particles typically subrounded or well rounded and well sorted; very thinly to very thickly bedded; contains planar and graded beds, cut-and-fill structures, trough and ripple crossbeds, and foresets, but also locally ranges to structureless. A northern source is indicated in a 35-ft-thick beach exposure north of Pleasant Harbor. Flame structures occur in the upper third of a 70-ft-thick, inaccessible exposure in the Dosewallips valley.
- Qgaf Vashon advance lacustrine silt and clay**—Glaciolacustrine silt and clay, locally with dropstones or interbeds of sand, pebbles, cobbles, or diamicton; gray; compact; typically well sorted; laminated to massive; 145 ft maximum thickness suggested by a well record in the Duckabush valley; mappable extent observed only in the Duckabush and Dosewallips valleys.

Pre-Vashon Olympic-sourced Glacial and Nonglacial Deposits, Undivided

- Qpuop Pre-Vashon alluvium**—Sandy to muddy pebble gravel, overbank (flood plain) or lacustrine sand and mud, scattered bits of charcoal and wood, localized gyttja seams; gray to orange-brown; compact; clasts angular to subangular; moderately sorted; bedded, with some mud beds as much as 1 ft thick seeming to lack internal bedding; observed thickness 6 ft; identified in one exposure in the Fulton Creek channel wall (date site GD4; Fig. A1) beneath 8 ft of post-Vashon alluvium (unit Qa); interpreted as pre-Vashon alluvium. We do not know enough about the timing of pre-Vashon pulses of Olympic alpine outwash to classify the deposit as glacial or nonglacial. The organic-rich character of the deposit suggests a nonglacial setting but does not exclude a glacial origin. Clasts are more angular than those in modern channel bedload, perhaps favoring glacial association.

Pre-Vashon Glacial Deposits

- Qapd Pre-Vashon Olympic-sourced glacial drift, undivided**—Till and outwash in a coarsening-upward sequence of sand to cobble and pebble gravel with sparse boulders and a typically brown to orange, clayey matrix (that may be the weathering product of a sandy matrix); typically marked by denser, more clayey matrix and more advanced weathering than Vashon deposits, but some exposures might be of Fraser age; faintly bedded or unbedded. Degrees of weathering and, south of the map area, stratigraphic relations suggest multiple Olympic ice advances over several hundred thousand years, as postulated by Carson (1980), who speculated on the presence of pre-Fraser but post-Salmon Springs Glaciation drift of Olympic source, and by Naeser and others (1984), Westgate and others (1987), Easterbrook and others (1988), Birdseye and Carson (1989), Polenz and others (2010a,b, 2012a,b), and Contreras and others (2010, 2012a,b). However, stratigraphic relations among exposures of unit Qapd in the map area are unresolved, and we did not observe a clear record of multiple Olympic ice advances. Unit Qapd is composed of more than 90 percent basalt in Fulton Creek basin (sec. 25, T25N R3W, and sec. 30, T25N R2W), the only part of the map area where surface exposures of mappable extent were recognized. Possible Olympic-sourced drift in parts of the Duckabush, Dosewallips, and Spencer Creek basins may have gone unrecognized because source areas would have included lower Crescent Formation and “core rocks” (Tabor and Cady, 1978) that would have been harder to differentiate compositionally from Vashon northern-sourced drift. Long (1975) mentioned Olympic till beneath Vashon Till in lower Rocky Brook valley and assigned it to the Evans Creek Stade of the Fraser Glaciation.
- Qpd Pre-Vashon northern-sourced glacial drift, undivided**—Till and outwash. Till: diamicton; medium to strong brown; compact; unstratified; partly weathered to secondary minerals; at least 13 ft thick along U.S. Highway 101, 700 ft north of the southern map edge; deposited directly by glacial ice and includes striated and faceted clasts. Outwash: sand and sandy pebble gravel; brown to gray; compact; subrounded to rounded clasts; moderately to well sorted; medium to thickly bedded; may be limited to the southern map edge, where it was inferred along the southwestern valley wall of Fulton Creek on the basis of

mapping of pre-Vashon drift by Contreras and others (2012a) to the south. Nearby exposures of stony sand may either be pockets of sand within the till or represent the unit's outwash facies.

Weathered northern-sourced drift, at least some of which is unit Qpd, has been noted at significant sites S10 to S16. At significant site S10 (midslope south of the lower Dosewallips River), Carson (1976) mapped a small patch of pre-Vashon drift ("Salmon Springs (?) till"). Diamicton in a roadcut beneath 3 to 7 ft of fresher Vashon Till at the site is mostly weathered to pale orange-brown clay, but inclusion of sparse unweathered basalt pebbles leads us to speculate that the deposit may be of Vashon age and derived mostly from proximally reworked unit Qpd, with much of the clay weathering thus inherited from pre-Vashon, northern-sourced drift concealed nearby. At a roadcut at significant site S11, we mapped 5 to 10 ft of brownish-gray, surficial till as Vashon Drift. Beneath this till, the roadcut exposed 10 ft of brownish-gray pebble gravel and cobbly diamicton. We did not characterize this as more weathered than the upsection till, but Frisken (1965) and Carson (1976) noted glaciolacustrine drift that they thought was too weathered to be of Vashon age. Frisken noted charcoal fragments suitable for radiocarbon analysis but did not obtain a date; we were unable to locate charcoal or lacustrine deposits and question whether the roadcut we saw in 2011 still revealed the pre-Vashon deposit. Granitic rocks mark deposits at S10 and S11 as northern sourced. At significant sites S12 to S16 (all located within 2.5 mi of the town of Brinnon), Carson (1976) mapped small exposures of pre-Vashon drift ("Salmon Springs (?) till"). We mapped surficial deposits in these areas as Vashon drift because we thought that their weathering was well within the range of weathering observed in Vashon Drift in the map area and much less severe than that of the older drift at S10. However, the Vashon cover in these areas is for the most part less than 10 ft thick and in places discontinuous. Carson may have identified older drift that we did not note beneath the surficial Vashon Drift. A wide range in the degree of weathering suggests that multiple glaciations may be included among pre-Vashon northern-sourced glacial deposits in the map area, and previous workers have advocated for such drifts elsewhere along the eastern Olympic mountains (Carson, 1980; Easterbrook and others, 1988; Birdseye and Carson, 1989; Kahle, 1998; Polenz and others, 2010a,b; Contreras and others, 2012a,c). A map boundary mismatch (sec. 30, T25N R2W) where Contreras and others (2012c) mapped "Glacial drift of MIS 6 (Double Bluff age)" has resulted because we did not agree that age control sufficed to infer that specific age.

Qpu Undivided Quaternary sediment older than Vashon Till—Sandy pebble gravel, sand, and sparse interbeds of mud; gray, with some light-brown mud beds and surficial iron staining; compact; exposed in foreset beds at the Quatsap Point delta (Bretz, 1913) west of Quatsap Point and in nearby lake-bottom sand beds along the east shore of Black Point; stratigraphically below Vashon Till, and appears to have been deposited by the ancestral Duckabush River. Parallel, west-dipping shears are discussed in the Structure section.

Rare andesite pebbles of apparent Cascade Range affinity are scattered in the (stratigraphically) upper half of the unit and are petrographically consistent with a single volcanic source but probably do not represent a single eruption (Michael Clynne, USGS, written commun., 2012). X-ray fluorescence (XRF) analysis of one such pebble from Quatsap Point (geochemistry site G1; Table E1) reveals a chemical signature that Clynne and Tom Sisson (USGS, written commun., 2012) could not associate with a known Puget Lowland tephra deposit. Sisson added that aspects of the chemistry and thin section petrography of the pebbles are, to his knowledge, not typical of any major Cascade volcano. Clynne noted that, despite some chemical affinity, Mount St. Helens provenance is geographically unlikely because the pebbles are not pumice. Affiliation with material from Glacier Peak is unlikely, given the petrographic character of the pebbles (Sisson and Clynne, written commun., 2012) and the XRF analytical signature of the Quatsap Point pebble (Table E2). Glacier Peak pebbles have been found in apparent lahar runout deposits as far southwest as central Whidbey Island (Table E2; Dragovich and others, 2005; Polenz and others, 2005, 2009b), but Clynne questions a Glacier Peak affiliation suggested by Contreras and others (2012b) for dacite pebbles along Hood Canal a few miles south of the map area. Small intrusive centers west of the main Cascade arc or Canadian provenance merit consideration as a source for the pebbles in the Brinnon quadrangle, especially in light of suggestions that the delta is associated with Cordilleran recessional-glacial conditions (see below). Preliminary review of chemical analyses of andesite mapped as Eocene at Anderson Lake near Port Townsend (25 mi north of Quatsap Point; Schasse and Slaughter, 2005) suggests that this andesite may be chemically compatible with the Quatsap Point pebble. The

Anderson Lake area is attractive as a source of the andesite pebbles in light of its proximity, and Vashon ice-flow lines suggest that Cordilleran ice could have moved material from there to Quatsap Point. The Washington State University Geoanalytical Laboratory is under contract to analyze the pebble by Inductively Coupled Plasma Mass Spectrometer (ICP-MS), and Sisson has a sample split that he plans to analyze by electron microprobe.

Rare inclusions in unit Qpu of granitic and high-grade metamorphic clasts and petrographic analysis of sand from unit Qpu indicate a greater fraction of northern-provenance material than found in modern Duckabush alluvium, but less than in the Vashon recessional Brinnon delta. This evidence and truncation of the delta foreset beds by lodgment till about 90 ft above modern sea level, an altitude comparable to the height and scale of the Brinnon delta, suggest association with a Cordilleran ice mass in the Puget Lowland, most likely during ice-mass recession (as asserted by Bretz, 1913); at that time, the Duckabush River would have drained into a proglacial lake and had access to ample northern-provenance material to add to its Olympic-provenance sediment. But the data also permit deposition during nonglacial conditions or Cordilleran ice advance.

Despite three new ~40 ka luminescence age estimates (date sites GD5 and GD6, Tables A1 and A2), the unit age is unresolved. Citing stratigraphic relations that we did not see during our field work in 2011, Bretz (1913) and Frisken (1965) interpreted the deposit as pre-Vashon, consistent with our perception that unit Qpu is more weathered than upsection unit Qgic. The luminescence data point to deposition during the Olympia nonglacial period but are poorly constrained. The presence of northern-provenance sediment favors Cordilleran glacial conditions. Comparison (Table A2) of our luminescence age estimates, those from the Brinnon delta, and radiocarbon-based age expectations for both sites suggests that all Quatsap Point and Black Point analyses may underestimate the true age to about the same degree as the Brinnon delta IRSL analysis. If indicative of a similar, systematic offset, this would favor a Vashon advance age (Table A2). Stratigraphic field relations noted by Bretz (1913) and the relative abundance of northern-provenance sediment with its implied bias toward Cordilleran ice-recessional conditions would suggest an early Wisconsinan (Possession Glaciation) or earlier age.

Qu Undivided Quaternary sediment (cross section only)—Undifferentiated deposits; may include boulders, cobbles, pebbles, sand, silt, clay, diamicton, and organic sediment; interpreted as sediment (instead of bedrock) from well records; compaction and stratigraphy suggest pre-Vashon age.

Tertiary Sedimentary and Volcanic Bedrock

Lower to middle Eocene Crescent Formation is the only bedrock observed in the map area. Overlying Tertiary marine sedimentary rocks in seemingly concordant contact with Crescent Formation are present north of the map area (Tabor and Cady, 1978; Al-Howar, 1990; Squires and others, 1992; Babcock and others, 1992a,b; Hirsch and Babcock, 2009) and south (Tabor and Cady, 1978; Contreras and others, 2010; Polenz and others, 2012a,b). Cady and others (1972), Tabor and Cady (1978), and Hirsch and Babcock (2009) divided the Crescent Formation into upper and lower members. The lower member (not noted in the map area) consists of marine basalt and massive diabasic flows, breccia, and sills, and interbeds of sandstone, siltstone, and limestone, all metamorphosed up to prehnite-pumpellyite facies. Metasomatism is common at the boundary between the lower and upper members. The upper member consists of subaerial columnar-jointed flows, mudflow breccia, and minor sedimentary interbeds.

Ev_c Crescent Formation—Mostly tholeiitic basalt, but ranges to basaltic trachyandesite (Table E3; Figs. E1 and E2); contains rare thin mudstone, siltstone, and sandstone interbeds between thick, subaerial, fine- to coarse-grained, blocky flows (Babcock and others, 1992a,b; Hirsch and Babcock, 2009); dark gray where fresh; gray, dark purple, or dark gray-green where weathered, commonly including green to white chlorite-group minerals, speckles of white amygdaloidal zeolite, or veins of quartz, calcite, and feldspar. Mineralogy typically includes plagioclase with intergrowths of augite and disseminated opaque minerals. Replacement of interstitial glass by chlorite and oxidation products is common. Sedimentary interbeds were seen only south of the Duckabush valley, where some bedrock includes pillow basalt and brecciated(?) textures—we suspect weathered tachylite or other basaltic glass. Such exposures dominate along South Fork Fulton Creek, where mudstone exposures are more extensive but not necessarily thicker than the 10-ft maximum observed elsewhere in the quadrangle.

Whole-rock analyses of 15 basalt samples (Table E3) reveal modest chemical variation and, as is typical of the Crescent Formation (Babcock and others, 1992a), trace element affinities to both mid-ocean ridge and intraplate lavas (Fig. E3). A trend from thick subaerial basalt flows in and north of the Duckabush valley to submarine basalt placement to the south (see also Contreras and others, 2010, 2012a,c; Polenz and others, 2012a,b) coincides with a change from less-differentiated flows (with higher contents of Cr and Mg) in the north to more-differentiated flows in the south (Fig. E4). The trend appears to continue southwest into the Eldon quadrangle, with additional chemical changes into the Hoodspout quadrangle (Fig. E4; Contreras and others, 2012a; Polenz and others, 2012a,b). Basalt flow stratigraphic and structural data within the Brinnon quadrangle are too sparse and varied to characterize these trends as either stratigraphic or geographic.

Elizabeth Nesbitt (Univ. of Wash., written commun., 2011) examined sedimentary rock samples from five sites (significant sites S18 to S21 and geochemistry site G16, all south of the Duckabush valley) and found no fossils that could constrain their age(s). A new ^{40}Ar - ^{39}Ar age estimate on basalt (date site G2) is 36.76 ± 0.32 Ma (Table A1), younger than generally expected of Crescent Formation but strikingly similar to a 36 Ma age estimate from 24 mi farther southwest (Polenz and others, 2012a,b). The sample is from about 1.25 mi east of where Cady and others (1972) and Tabor and Cady (1978) mapped the contact between the upper and lower members of the Crescent Formation, suggesting that it represents the lower third of the upper member of the Crescent Formation, stratigraphically between prior age-estimates for the top and base of the upper Crescent Formation (Hirsch and Babcock, 2009). The exact position along Hirsch and Babcock's section is hard to determine, in part due to apparent structural complexity (see Structure section). A map-edge mismatch has resulted where Contreras and others (2012a) mapped Olympic-sourced outwash east of Fulton Creek; basalt bedrock dominates the steep hill on the Brinnon quadrangle side.

ACKNOWLEDGMENTS

This geologic map was funded in part by the USGS National Cooperative Geologic Mapping Program under award no. G11AC20236. We thank the Jefferson County Assessor's Office for GIS data; Rex Crawford (DNR, Natural Heritage Program) for tree cone species identification; Rick Blakely and Tom Pratt (both USGS) for seismic and aeromagnetic data; Andy Lamb (Boise State Univ.) for magnetic and seismic line data and assistance with its interpretation; Brian Sherrod (USGS) for marine magnetic data and biostratigraphic analysis of estuarine sediment samples; Scott Babcock, David Hirsch (both Western Wash. Univ.), and Emily Lindstrum (Univ. of Hawaii) for previously unpublished information regarding their published age-control data; Tom Sisson and Michael Clynne (both USGS), and Pat Pringle (Centralia College) for assistance with analysis and interpretation of volcanic clasts from pre-Vashon sediment; Paul Bakke (U.S. Fish and Wildlife Service) for assistance with assessment of Dosewallips River system behavior and interpretation of records used in cross-section development; Elizabeth Nesbitt (Burke Museum of Natural History and Culture, Univ. of Wash.) for assistance with processing and stratigraphic interpretation of sedimentary rocks; Mark Bruskiewicz (WSDOT) for assistance with climatic record metadata; Ken Craeger and Tom Yelin (Pacific Northwest Seismic Network, Univ. of Wash.) for earthquake records and processing thereof; Anne Marshall (Wash. Dept. of Fish and Wildlife) and Pat Martin for assistance with assessment of salmonid genealogy and its implications for glacial history of the map area; Glenn Thackray (Idaho State Univ.) and Wendy Gerstel (Qwg Applied Geology) for insights into glaciations of the Olympic Mountains; Mac McKay (DNR) for assistance with interpretation of a paleoenvironmental setting; Trevor Contreras, Joe Dragovich, and Jessica Czajkowski (all Wash. Div. of Geology and Earth Resources) for reviews and assistance with interpretation of aspects of this mapping; and Pope Resources, the U.S. Forest Service, George Houdeck, Richard Arkless, Bob Herbst, and many others for sharing local knowledge and permitting us to map on their land, and Gary Petro (DNR) for a helpful pre-publication review.

REFERENCES CITED

- Al-Howar, Saad, 1990, Upper Eocene fossils from sediments west of Dabob Bay, Washington: University of Puget Sound Bachelor of Science thesis, 31 p.
- Anderson, M. L.; Dragovich, J. D.; Blakely, R. J.; Wells, R. E.; Brocher, T. M., 2008, Where does the Seattle fault end?—Structural links and kinematic implication [abstract]: *Eos (American Geophysical Union Transactions)*, v. 89, no. 53, Suppl., p. F2535-F2536.
- Atwater, B. F., 1999, Radiocarbon dating of a Seattle earthquake to A.D. 900-930 [abstract]: *Seismological Research Letters*, v. 70, no. 2, p. 232.
- Babcock, R. S.; Burmester, R. F.; Engebretson, D. C.; Warnock, A. C.; Clark, K. P., 1992a, A rifted margin origin for the Crescent basalts and related rocks in the northern Coast Range volcanic province, Washington and British Columbia: *Journal of Geophysical Research*, v. 97, no. B5, p. 6799-6821.
- Babcock, R. S.; Suczek, C. A.; Engebretson, D. C., 1992b, Geology of the Crescent terrane, Olympic Peninsula, WA [abstract]: *Geological Society of America Abstracts with Programs*, v. 24, no. 5, p. 4.
- Bilderback, E. L.; Palmer, S. P.; Folger, D. S.; Poelstra, J. L.; Magsino, S. L.; Niggemann, R. A., 2008, Shear-wave database for Quaternary and bedrock geologic units, Washington State: Washington Division of Geology and Earth Resources Open File Report 2008-2, 528 p., with CD of database and 3 text files. [http://www.dnr.wa.gov/Publications/ger_ofr2008-2_shear_wave_database.zip]
- Birdseye, R. U.; Carson, R. J., 1989, Tephra of Salmon Springs age from the southeastern Olympic Peninsula, Washington: Washington Division of Geology and Earth Resources Open File Report 74-1 (revised), 23 p. [http://www.dnr.wa.gov/publications/ger_ofr74-1_tephra_olympic_peninsula.pdf]
- Blakely, R. J.; Sherrod, B. L.; Hughes, J. F.; Anderson, M. L.; Wells, R. E.; Weaver, C. S., 2009, Saddle Mountain fault deformation zone, Olympic Peninsula, Washington—Western boundary of the Seattle uplift: *Geosphere*, v. 5, no. 2, p. 105-125.
- Blakely, R. J.; Wells, R. E.; Weaver, C. S.; Johnson, S. Y., 2002, Location, structure, and seismicity of the Seattle fault zone, Washington—Evidence from aeromagnetic anomalies, geologic mapping, and seismic-reflection data: *Geological Society of America Bulletin*, v. 114, no. 2, p. 169-177.
- Booth, D. B.; Troost, K. G.; Clague, J. J.; Waitt, R. B., 2004, The Cordilleran ice sheet. *In* Gillespie, A. R.; Porter, S. C.; Atwater, B. F., editors, *The Quaternary period in the United States*: Elsevier, p. 17-43.
- Bretz, J. H., 1913, Glaciation of the Puget Sound region: *Washington Geological Survey Bulletin* 8, 244 p., 3 plates. [http://www.dnr.wa.gov/publications/ger_b8_glaciation_pugetsound.pdf]
- Brocher, T. M.; Parsons, T. E.; Blakely, R. J.; Christensen, N. I.; Fisher, M. A.; Wells, R. E.; SHIPS Working Group, 2001, Upper crustal structure in Puget Lowland, Washington—Results from the 1998 Seismic Hazards Investigations in Puget Sound: *Journal of Geophysical Research*, v. 106, no. B7, p. 13,541-13,564.
- Bucknam, R. C.; Hemphill-Haley, Eileen; Leopold, E. B., 1992, Abrupt uplift within the past 1700 years at southern Puget Sound, Washington: *Science*, v. 258, no. 5088, p. 1611-1614.
- Cady, W. M.; Sorensen, M. L.; MacLeod, N. S., 1972, Geologic map of the Brothers quadrangle, Jefferson, Mason and Kitsap Counties, Washington: U.S. Geological Survey Geologic Quadrangle Map GQ-969, 1 sheet, scale 1:62,500. [http://ngmdb.usgs.gov/Prodesc/proddesc_2268.htm]
- Carson, R. J., 1973, First known active fault in Washington: *Washington Geologic Newsletter*, v. 1, no. 3, p. 1-2. [http://www.dnr.wa.gov/Publications/ger_washington_geology_1973_v1_no3.pdf]
- Carson, R. J., 1976, Preliminary geologic map of the Brinnon area, Jefferson County, Washington: Washington Division of Geology and Earth Resources Open File Report 76-3, 1 sheet, scale 1:24,000. [http://www.dnr.wa.gov/publications/ger_ofr76-3_geol_map_brinnon_24k.pdf]
- Carson, R. J., 1980, Quaternary, environmental, and economic geology of the eastern Olympic Peninsula, Washington: [unpublished report], 275 p.
- Contreras, T. A.; Legorreta Paulin, Gabriel; Czajkowski, J. L.; Polenz, Michael; Logan, R. L.; Carson, R. J.; Mahan, S. A.; Walsh, T. J.; Johnson, C. N.; Skov, R. H., 2010, Geologic map of the Lilliwaup 7.5-minute quadrangle, Mason County, Washington: Washington Division of Geology and Earth Resources Open File Report 2010-4, 13 p., 1 plate, scale 1:24,000. [http://www.dnr.wa.gov/Publications/ger_ofr2010-4_geol_map_lilliwaup_24k.zip]

- Contreras, T. A.; Spangler, Eleanor; Fusso, L. A.; Reiou, D. A.; Legorreta Paulin, Gabriel; Pringle, P. T.; Carson, R. J.; Lindstrum, E. F.; Clark, K. P.; Tepper, J. H.; Pileggi, Domenico; Mahan, S. A., 2012a, Geologic map of the Eldon 7.5-minute quadrangle, Jefferson, Kitsap, and Mason Counties, Washington: Washington Division of Geology and Earth Resources Map Series 2012-03, 1 sheet, scale 1:24,000, plus 60 p. text. [http://www.dnr.wa.gov/Publications/ger_ms2012-03_geol_map_eldon_24k.zip]
- Contreras, T. A.; Weeks, S. A.; Perry, B. B., 2012b, Analytical data from the Holly 7.5-minute quadrangle, Jefferson, Kitsap, and Mason Counties, Washington—Supplement to Open File Report 2011-5: Washington Division of Geology and Earth Resources Open File Report 2011-6, 16 p. [http://www.dnr.wa.gov/Publications/ger_ofr2011-6_holly_supplement.pdf]
- Contreras, T. A.; Weeks, S. A.; Stanton, K. M. D.; Stanton, B. W.; Perry, B. B.; Walsh, T. J.; Carson, R. J.; Clark, K. P.; Mahan, S. A., 2012c, Geologic map of the Holly 7.5-minute quadrangle, Jefferson, Kitsap, and Mason Counties, Washington: Washington Division of Geology and Earth Resources Open File Report 2011-5, 1 sheet, scale 1:24,000, 13 p. text. [http://www.dnr.wa.gov/Publications/ger_ofr2011-5_geol_map_holly_24k.zip]
- Crandell, D. R., 1964, Pleistocene glaciations of the southwestern Olympic Peninsula, Washington: U.S. Geological Survey Professional Paper 501-B, p. B135-B139.
- Czajkowski, J. L.; Walsh, T. J.; Contreras, T. A.; Davis-Stanton, Kelsay; Kelsey, H. M.; Schermer, E. R.; Carson, R. J., 2009, Active faulting along a segment of the Saddle Mountain fault zone, southeastern Olympic Mountains, WA—A paleoseismic trenching study [abstract]. *In* Northwest Scientific Association, The Pacific Northwest in a changing environment—Northwest Scientific Association 81st annual meeting; Program with abstracts: Northwest Scientific Association, p. 14.
- Daneš, Z. F., 1985, Sedimentary thickness in the Puget Sound area, Washington, derived from aeromagnetic data: Washington Division of Geology and Earth Resources Open File Report 85-5, 14 p. [http://www.dnr.wa.gov/publications/ger_ofr85-5_puget_sound_sediment_thickness.pdf]
- Daneš, Z. F.; Bonno, M.; Brau, J. E.; Gilham, W. D.; Hoffman, T. F.; Johansen, D.; Jones, M. H.; Malfait, Bruce; Masten, J.; Teague, G. O., 1965, Geophysical investigation of the southern Puget Sound area, Washington: *Journal of Geophysical Research*, v. 70, no. 22, p. 5573-5580.
- Dragovich, J. D.; Petro, G. T.; Thorsen, G. W.; Larson, S. L.; Foster, G. R.; Norman, D. K., 2005, Geologic map of the Oak Harbor, Crescent Harbor, and part of the Smith Island 7.5-minute quadrangles, Island County, Washington: Washington Division of Geology and Earth Resources Geologic Map GM-59, 2 sheets, scale 1:24,000. [http://www.dnr.wa.gov/Publications/ger_gm59_geol_map_oakharbor_crescentharbor_24k.zip]
- Dragovich, J. D.; Pringle, P. T.; Walsh, T. J., 1994, Extent and geometry of the mid-Holocene Osceola mudflow in the Puget Lowland—Implications for Holocene sedimentation and paleogeography: *Washington Geology*, v. 22, no. 3, p. 3-26. [http://www.dnr.wa.gov/Publications/ger_washington_geology_1994_v22_no3.pdf]
- Easterbrook, D. J.; Roland, J. L.; Carson, R. J.; Naeser, N. D., 1988, Application of paleomagnetism, fission-track dating, and tephra correlation to lower Pleistocene sediments in the Puget Lowland, Washington. *In* Easterbrook, D. J., editor, *Dating Quaternary sediments: Geological Society of America Special Paper 227*, p. 139-165.
- Friskien, J. G., 1965, Pleistocene glaciation of the Brinnon area, east-central Olympic Peninsula, Washington: University of Washington Master of Science thesis, 75 p., 3 plates.
- Garcia, A. F., 1996, Active tectonic deformation and late Pleistocene and Holocene geomorphic and soil profile evolution in the Dosewallips River drainage basin, Olympic Mountains, western Washington State: University of New Mexico Master of Science thesis, 152 p., 4 plates.
- Gavin, D. G., 2001, Estimation of inbuilt age in radiocarbon ages of soil charcoal for fire history studies: *Radiocarbon*, v. 43, no. 1, p. 27-44.
- Gerstel, W. J.; Lingley, W. S., Jr., 2003, Geologic map of the Mount Olympus 1:100,000 quadrangle, Washington: Washington Division of Geology and Earth Resources Open File Report 2003-4, 1 sheet, scale 1:100,000. [http://www.dnr.wa.gov/Publications/ger_ofr2003-4_geol_map_mountolympus_100k.pdf]
- Glassley, W. E., 1974, Geochemistry and tectonics of the Crescent volcanic rocks, Olympic Peninsula, Washington: *Geological Society of America Bulletin*, v. 85, no. 5, p. 785-794.
- Grimstad, Peder; Carson, R. J., 1981, Geology and ground-water resources of eastern Jefferson County, Washington: Washington Department of Ecology Water-Supply Bulletin 54, 125 p., 3 plates. [http://www.ecy.wa.gov/programs/eap/wsb/wsb_All.html#p54]
- Haug, B. J., 1998, High resolution seismic reflection interpretations of the Hood Canal–Discovery Bay fault zone; Puget Sound, Washington: Portland State University Master of Science thesis, 1 v.
- Haugerud, R. A., 2005, Preliminary geologic map of Bainbridge Island, Washington: U.S. Geological Survey Open-File Report 2005-1387, version 1.0, 1 sheet, scale 1:24,000. [<http://pubs.usgs.gov/of/2005/1387>]

- Haugerud, R. A., 2009, Preliminary geomorphic map of the Kitsap Peninsula, Washington; version 1.0: U.S. Geological Survey Open-File Report 2009-1033, 2 sheets, scale 1:36,000. [<http://pubs.usgs.gov/of/2009/1033/>]
- Hellwig, J. L., 2010, The interaction of climate, tectonics, and topography in the Olympic Mountains of Washington State—The influence of erosion on tectonic steady-state and the synthesis of the alpine glacial history: University of Illinois at Urbana-Champaign Masters thesis, 335 p.
- Hirsch, D. M.; Babcock, R. S., 2009, Spatially heterogeneous burial and high-P/T metamorphism in the Crescent Formation, Olympic Peninsula, Washington: *American Mineralogist*, v. 94, no. 8-9, p. 1103-1110.
- Hughes, J. F., 2005, Meters of synchronous Holocene slip on two strands of a fault in the western Puget Sound Lowland, Washington [abstract]: *Eos (American Geophysical Union Transactions)*, v. 86, no. 52, p. F1437.
- Irvine, T. N.; Baragar, W. R. A., 1971, A guide to the chemical classification of the common volcanic rocks: *Canadian Journal of Earth Sciences*, p. 523-548
- Jones, M. A., 1996, Thickness of unconsolidated deposits in the Puget Sound lowland, Washington and British Columbia: U.S. Geological Survey Water-Resources Investigations Report 94-4133, 1 sheet. [<http://pubs.er.usgs.gov/usgspubs/wri/wri944133>]
- Johnson, S. Y.; Blakely, R. J.; Stephenson, W. J.; Dadisman, S. V.; Fisher, M. A., 2004, Active shortening of the Cascadia forearc and implications for seismic hazards of the Puget Lowland: *Tectonics*, v. 23, TC1011, doi:10.1029/2003TC001507, 27 p.
- Kahle, S. C., 1998, Hydrogeology of Naval Submarine Base Bangor and vicinity, Kitsap County, Washington: U.S. Geological Survey Water-Resources Investigations Report 97-4060, 107 p., 7 plates. [<http://pubs.er.usgs.gov/usgspubs/wri/wri974060>]
- Karel, Patrick; Liberty, L. M., 2008, The western extension of the Seattle fault—New insights from seismic reflection data: American Geophysical Union Fall Meeting 2008, poster T21B-1951.
- Kelsey, H. M.; Sherrod, B. L.; Nelson, A. R.; Brocher, T. M., 2008, Earthquakes generated from bedding plane-parallel reverse faults above an active wedge thrust, Seattle fault zone: *Geological Society of America Bulletin*, v. 120, no. 11-12, p. 1581-1597.
- Koppers, A. A. P.; Staudigel, Hubert; Duncan, R. A., 2003, High-resolution $^{40}\text{Ar}/^{39}\text{Ar}$ dating of the oldest oceanic basement basalts in the western Pacific basin: *Geochemistry Geophysics Geosystems*, v. 4, no. 11, p. 1-20.
- Kramer, S. L., 1996, *Geotechnical earthquake engineering*: Prentice Hall, 653 p.
- Lamb, A. P.; Liberty, L. M.; Blakely, R. J.; Pratt, T. L.; Sherrod, B. L.; van Wijk, K., 2012, Western limits of the Seattle fault zone and its interaction with the Olympic Peninsula, Washington: *Geosphere*, v. 8, no. 3, doi: 10.1130/GESoo780.1.
- Lamb, A. P.; Liberty, L. M.; Blakely, R. J.; van Wijk, Kasper, 2009a, The Dewatto lineament—Southwestern extension of the Seattle fault? [poster for] The Tahuya lineament—Southwestern extension of the Seattle fault? [abstract]: *Geological Society of America Abstracts with Programs*, v. 41, no. 7, p. 479.
- Lamb, A. P.; Liberty, L. M.; Blakely, R. J.; van Wijk, Kasper, 2009b, The Tahuya lineament—Southwestern extension of the Seattle fault? [abstract]: *Geological Society of America Abstracts with Programs*, v. 41, no. 7, p. 479.
- Lane, J. W., Jr.; White, E. A.; Steele, G. V.; Cannia, J. C., 2008, Estimation of bedrock depth using the horizontal-to-vertical (H/V) ambient-noise seismic method. *In* Symposium on the Application of Geophysics to Engineering and Environmental Problems, April 6-10, 2008, Philadelphia, Pennsylvania, Proceedings: Denver, Colorado, Environmental and Engineering Geophysical Society, 13 p., [http://water.usgs.gov/ogw/bgas/publications/SAGEEP2008-Lane_HV/SAGEEP2008-Lane_HV.pdf]
- Laprade, W. T., 2003, Subglacially reworked till in the Puget Lowland [abstract]: *Geological Society of America Abstracts with Programs*, v. 35, no. 6, p. 216.
- Le Bas, M. J.; Le Maitre, R. W.; Streckeisen, A.; Zanettin, B., 1986, A chemical classification 627 of volcanic rocks based on the total alkali silica diagram: *Journal of Petrology*, v. 27, p. 745-750.
- Liberty, L. M.; Pratt, T. L., 2008, Structure of the eastern Seattle fault zone, Washington State—New insights from seismic reflection data: *Bulletin of the Seismological Society of America*, v. 98, no. 4, p. 1681-1695.
- Lindstrum, E. F., 2002, Stratigraphic analysis of Holocene deltaic deposits on the western margin of the Puget Lowland, Hood Canal, Washington: University of Oregon Master of Science thesis, 77 p.
- Logan, R. L.; Walsh, T. J., 2009, Mima Mounds formation and their implications for climate change [abstract]. *In* Northwest Scientific Association, The Pacific Northwest in a changing environment—Northwest Scientific Association 81st annual meeting; Program with abstracts: Northwest Scientific Association, p. 38-39.
- Long, W. A., 1974, Glacial geology of the northeastern Olympic Mountains, Washington: U.S. Forest Service, 129 p.
- Long, W. A., 1975, Glacial studies on the Olympic Peninsula: U.S. Forest Service, 1 v., 9 plates.

- Long, W. A., 1976, Glacial geology of the eastern Olympic Peninsula, Washington. *In* Glacial geology of the Olympic Peninsula: U.S. Forest Service, 23 p., 2 plates.
- Mace, C. G.; Keranen, K. M., 2012, Oblique fault systems crossing the Seattle basin—Geophysical evidence for additional shallow fault systems in the central Puget Lowland: *Journal of Geophysical Research*, v. 117, B03105, 19 p.
- Martin, M. E.; Maxcia, Claudia; Gerardi, Flavia; Bourgeois, Joanne, 2007, Anomalous sand deposit associated with evidence of late Holocene uplift near Bremerton, Washington [abstract]: *Eos (American Geophysical Union Transactions)*, v. 88, no. 52, pt. 2, Supplement, p. F1433.
- Mosher, D. C.; Hewitt, A. T., 2004, Late Quaternary deglaciation and sea-level history of eastern Juan de Fuca Strait, Cascadia: *Quaternary International*, v. 121, no. 1, p. 23-39.
- Mullen, E. D., 1983, MnO/TiO₂/P₂O₅—A minor element discriminant for basaltic rocks of oceanic environments and its implications for petrogenesis: *Earth and Planetary Science Letters*, v. 62, p. 53-62.
- Naeser, N. D.; Westgate, J. A.; Easterbrook, D. J.; Carson, R. J., 1984, Pre-0.89 my glaciation in the west central Puget Lowland, Washington [abstract]: *Geological Society of America Abstracts with Programs*, v. 16, no. 5, p. 324.
- Nelson, A. R.; Johnson, S. Y.; Kelsey, H. M.; Sherrod, B. L.; Wells, R. E.; Okumura, Koji; Bradley, Lee-Ann; Bogar, Robert; Personius, S. F., 2003a, Field and laboratory data from an earthquake history study of the Waterman Point fault, Kitsap County, Washington: U.S. Geological Survey Miscellaneous Field Studies Map MF-2423, 1 sheet, scale 1:3,000, with [11 p. text]. [<http://pubs.usgs.gov/mf/2003/mf-2423>]
- Nelson, A. R.; Johnson, S. Y.; Kelsey, H. M.; Wells, R. E.; Sherrod, B. L.; Pezzopane, S. K.; Bradley, Lee-Ann; Koehler, R. D., III; Bucknam, R. C., 2003b, Late Holocene earthquakes on the Toe Jam Hill fault, Seattle fault zone, Bainbridge Island, Washington: *Geological Society of America Bulletin*, v. 115, no. 11, p. 1388-1403.
- Nelson, A. R.; Johnson, S. Y.; Wells, R. E.; Pezzopane, S. K.; Kelsey, H. M.; Sherrod, B. L.; Bradley, Lee-Ann; Koehler, R. D., III; Bucknam, R. C.; Haugerud, R. A.; Laprade, W. T., 2002, Field and laboratory data from an earthquake history study of the Toe Jam Hill fault, Bainbridge Island, Washington: U.S. Geological Survey Open-File Report 02-60, 1 v., 2 plates. [<http://pubs.usgs.gov/of/2002/ofr-02-0060/>]
- Nelson, A. R.; Sherrod, B. L.; Johnson, S. Y.; Kelsey, H. M.; Wells, R. E.; Pezzopane, S. K.; Bradley, L. A.; Koehler, R. D.; Bogar, Robert; Okumura, Koji, 2003c, Earthquake history of reverse faults and folds in trenches across ALSM-imaged scarps in the Seattle fault zone, Puget Lowland, Washington State [abstract]: *International Union for Quaternary Research, XVI INQUA Congress—Shaping the Earth, a Quaternary perspective*, p. 108. [http://www.inqua2003.dri.edu/inqua03_abstracts_p101-124.pdf]
- Parker, D. F.; Hodges, F. N.; Perry, A.; Mitchener, M. E.; Barnes, M. A.; Ren, M., 2010, Geochemistry and petrology of late Eocene Cascade Head and Yachats Basalt and alkalic intrusions of the central Oregon Coast Range, U.S.A.: *Journal of Volcanology and Geothermal Research*, v. 198, Issues 3-4, p. 311-324.
- Pettijohn, F. J., 1957, *Sedimentary rocks*: Harper and Brothers, 718 p.
- Polenz, Michael; Alldritt, Katelin; Heheman, N. J.; Sarikhan, I. Y.; Logan, R. L., 2009a, Geologic map of the Belfair 7.5-minute quadrangle, Mason, Kitsap, and Pierce Counties, Washington: Washington Division of Geology and Earth Resources Open File Report 2009-7, 1 sheet, scale 1:24,000. [http://www.dnr.wa.gov/Publications/ger_ofr2009-7_geol_map_belfair_24k.pdf]
- Polenz, Michael; Contreras, T. A.; Czajkowski, J. L.; Legorreta Paulin, Gabriel; Miller, B. A.; Martin, M. E.; Walsh, T. J.; Logan, R. L.; Carson, R. J.; Johnson, C. N.; Skov, R. H.; Mahan, S. A.; Cohan, C. R. 2010a, Supplement to geologic maps of the Lilliwaup, Skokomish Valley, and Union 7.5-minute quadrangles, Mason County, Washington—Geologic setting and development around the Great Bend of Hood Canal: Washington Division of Geology and Earth Resources Open File Report 2010-5, 27 p. [http://www.dnr.wa.gov/Publications/ger_ofr2010-5_lilliwaup_skokomish_valley_union_suppl_24k.pdf]
- Polenz, Michael; Czajkowski, J. L.; Legorreta Paulin, Gabriel; Contreras, T. A.; Miller, B. A.; Martin, M. E.; Walsh, T. J.; Logan, R. L.; Carson, R. J.; Johnson, C. N.; Skov, R. H.; Mahan, S. A.; Cohan, C. R., 2010b, Geologic map of the Skokomish Valley and Union 7.5-minute quadrangles, Mason County, Washington: Washington Division of Geology and Earth Resources Open File Report 2010-3, 21 p., 1 plate, scale 1:24,000. [http://www.dnr.wa.gov/Publications/ger_ofr2010-3_geol_map_skokomish_valley_union_24k.zip]
- Polenz, Michael; Miller, B. A.; Davies, Nigel; Perry, B. B.; Clark, K. P.; Walsh, T. J.; Carson, R. J.; Hughes, J. F., 2012a, Geologic map of the Hoodspport 7.5-minute quadrangle, Mason County, Washington: Washington Division of Geology and Earth Resources Open File Report 2011-3, 1 sheet, scale 1:24,000, 18 p. text. [http://www.dnr.wa.gov/Publications/ger_ofr2011-3_geol_map_hoodspport_24k.zip]
- Polenz, Michael; Miller, B. A.; Davies, Nigel; Perry, B. B.; Hughes, J. F.; Clark, K. P.; Walsh, T. J.; Tepper, J. H.; Carson, R. J., 2012b, Analytical data from the Hoodspport 7.5-minute quadrangle, Mason County, Washington—Supplement to Open File Report 2011-3: Washington Division of Geology and Earth Resources Open File Report 2011-4, 42 p. [http://www.dnr.wa.gov/Publications/ger_ofr2011-4_hoodspport_supplement.pdf]

- Polenz, Michael; Schasse, H. W.; Kalk, M. L.; Petersen, B. B., 2009b, Geologic map of the Camano 7.5-minute quadrangle, Island County, Washington: Washington Division of Geology and Earth Resources Geologic Map GM-68, 1 sheet, scale 1:24,000. [http://www.dnr.wa.gov/Publications/ger_gm68_geol_map_camano_24k.pdf]
- Polenz, Michael; Slaughter, S. L.; Thorsen, G. W., 2005, Geologic map of the Coupeville and part of the Port Townsend North 7.5-minute quadrangles, Island County, Washington: Washington Division of Geology and Earth Resources Geologic Map GM-58, 1 sheet, scale 1:24,000. [http://www.dnr.wa.gov/Publications/ger_gm58_geol_map_coupeville_24k.pdf]
- Porter, S. C.; Carson, R. J., 1971, Problems of interpreting radiocarbon dates from dead-ice terrain, with an example from the Puget Lowland of Washington: *Quaternary Research*, v. 1, no. 3, p. 410-414.
- Porter, S. C.; Swanson, T. W., 1998, Radiocarbon age constraints on rates of advance and retreat of the Puget lobe of the Cordilleran ice sheet during the last glaciation: *Quaternary Research*, v. 50, no. 3, p. 205-213.
- Pratt, Thomas; Troost, Kathy, 2009, Is the Seattle fault beneath downtown Seattle? [abstract]. In Northwest Scientific Association, The Pacific Northwest in a changing environment—Northwest Scientific Association 81st annual meeting; Program with abstracts: Northwest Scientific Association, p. 53-54.
- Prescott, J. R.; Hutton, J. T., 1994, Cosmic ray contribution to dose rates for luminescence and ESR dating—Large depths and long-term time variations: *Radiation Measurements*, v. 23, no. 2-3, p. 497-500.
- Raisz, E. J., 1945, The Olympic-Wallowa lineament: *American Journal of Science*, v. 243A [Daly volume], p. 479-485. [<http://earth.geology.yale.edu/~ajs/1945A/479.pdf>]
- Renne, P. R.; Deino, A. L.; Walter, R. C.; Turrin, B. D.; Swisher III, C. C.; Becker, T. A.; Curtis, G. H.; Sharp, W. D.; Jaouni, A. R., 1994, Intercalibration of astronomical and radioisotopic time: *Geology*, v. 22, p. 783-786.
- Rhodes, E. J., 2011, Optically stimulated luminescence dating of sediments over the past 200,000 years: *Annual Review of Earth and Planetary Sciences*, v. 39, p. 461-488.
- Robinson, J. W., 1938, The general geology of the Lake Cushman and Hama Hama River area of the Olympic Mountains: University of Washington Bachelor of Science thesis, 32 p.
- Rogers, W. P., 1970, A geological and geophysical study of the central Puget Sound lowland: University of Washington Doctor of Philosophy thesis, 123 p., 9 plates.
- Sarikhan, I. Y.; Stanton, K. D.; Contreras, T. A.; Polenz, Michael; Powell, Jack; Walsh, T. J.; Logan, R. L., 2008, Landslide reconnaissance following the storm event of December 1–3, 2007, in western Washington: Washington Division of Geology and Earth Resources Open File Report 2008-5, 16 p. [http://www.dnr.wa.gov/Publications/ger_ofr2008-5_dec2007_landslides.pdf]
- Schasse, H. W.; Slaughter, S. L., 2005, Geologic map of the Port Townsend South and part of the Port Townsend North 7.5-minute quadrangles, Jefferson County, Washington: Washington Division of Geology and Earth Resources Geologic Map GM-57, 1 sheet, scale 1:24,000. [http://www.dnr.wa.gov/Publications/ger_gm57_geol_map_porttownsends_24k.pdf]
- Shannon & Wilson, Inc., 1998, Geotechnical report—Dosewallips bridge replacement, SR-101, Jefferson County, Washington: Washington State Department of Transportation, 1 v.
- Squires, R. L.; Goedert, J. L.; Kaler, K. L., 1992, Paleontology and stratigraphy of Eocene rocks at Pulali Point, Jefferson County, eastern Olympic Peninsula, Washington: Washington Division of Geology and Earth Resources Report of Investigations 31, 27 p. [http://www.dnr.wa.gov/publications/ger_ri31_eocene_rock_jefferson_county.pdf]
- Tabor, R. W.; Cady, W. M., 1978, Geologic map of the Olympic Peninsula, Washington: U.S. Geologic Survey Miscellaneous Investigations Series Map I-994, 2 sheets, scale 1:125,000.
- Tabor, R. W.; Haugerud, R. A.; Haeussler, P. J.; Clark, K. P., 2011, Lidar-revised geologic map of the Wildcat Lake 7.5' quadrangle, Kitsap and Mason Counties, Washington: U.S. Geological Survey Scientific Investigations Map 3187, 2 sheets, scale 1:24,000, with 12 p. text. [<http://pubs.usgs.gov/sim/3187>]
- Thackray, G. D., 2001, Extensive early and middle Wisconsin glaciation on the western Olympic Peninsula, Washington, and the variability of Pacific moisture delivery to the northwestern United States: *Quaternary Research*, v. 55, no. 3, p. 257-270.
- Thorson, R. M., 1980, Ice-sheet glaciation of the Puget Lowland, Washington, during the Vashon Stade (late Pleistocene): *Quaternary Research*, v. 13, no. 3, p. 303-321.
- Thorson, R. M., 1981, Isostatic effects of the last glaciation in the Puget Lowland, Washington: U.S. Geological Survey Open-File Report 81-370, 100 p., 1 plate. [Text: http://pubs.er.usgs.gov/djvu/OFR/1981/ofr_81_370.djvu; Plate: http://pubs.er.usgs.gov/djvu/OFR/1981/ofr_81_370_plt.djvu]
- Thorson, R. M., 1989, Glacio-isostatic response of the Puget Sound area, Washington: *Geological Society of America Bulletin*, v. 101, no. 9, p. 1163-1174.
- Todd, M. R., 1939, The glacial geology of the Hamma Hamma Valley and its relation to the glacial history of the Puget Sound basin: University of Washington Master of Science thesis, 48 p., 1 plate.

- U.S. Geological Survey Geologic Names Committee, 2010, Divisions of geologic time—Major chronostratigraphic and geochronologic units: U.S. Geological Survey Fact Sheet 2010-3059, 2 p. [<http://pubs.usgs.gov/fs/2010/3059/>]
- Westgate, J. A.; Easterbrook, D. J.; Naeser, N. D.; Carson, R. J., 1987, Lake Tapps tephra—An early Pleistocene stratigraphic marker in the Puget Lowland, Washington: *Quaternary Research*, v. 28, no. 3, p. 340-355.
- Wilson, J. R., 1975, Geology of the Price Lake area, Mason County, Washington: North Carolina State University Master of Science thesis, 79 p., 2 plates.
- Wilson, J. R.; Bartholomew, M. J.; Carson, R. J., 1979, Late Quaternary faults and their relationship to tectonism in the Olympic Peninsula, Washington: *Geology*, v. 7, no. 5, p. 235-239.
- Witter, R. C.; Givler, R. W., 2005, Two post-glacial earthquakes on the Saddle Mountain West fault, southeastern Olympic Peninsula, Washington: U.S. Geological Survey, National Earthquake Hazards Reduction Program Final Technical Report, Award No. 05HQGR0089, [50 p.]. [<http://earthquake.usgs.gov/research/external/reports/05HQGR0089.pdf>]
- Witter, R. C.; Givler, R. W.; Carson, R. J., 2008, Two post-glacial earthquakes on the Saddle Mountain west fault, southeastern Olympic Peninsula, Washington: *Bulletin of the Seismological Society of America*, v. 98, no. 6, p. 2894-2917.
- Yount, J. C.; Gower, H. D., 1991, Bedrock geologic map of the Seattle 30' by 60' quadrangle, Washington: U.S. Geological Survey Open-File Report 91-147, 37 p., 4 plates. [<http://pubs.er.usgs.gov/usgspubs/ofr/ofr91147>]

Appendix A. Age Control Data



Figure A1. Alluvium of unit Qpu_{op} at date site GD4. The Fulton Creek channel cutbank exposes compact, Olympic-sourced sediment. Wood fragments from the gray mud near the lower half of the pick handle (and also present in the gray mud above the pick) yielded a 19,600 ±80 yr BP radiocarbon date (Table A1), demonstrating a pre-Vashon age for the alluvium. The orange patches in the gray mud are surficial; the uniformly gray to bluish-gray mud deeper in the bank provided an anoxic sample host environment for the radiocarbon sample even at the time of sampling during a drier part of the year, early August 2011. It is unclear if the deposit is best interpreted as Olympic glacial outwash or nonglacial Olympic alluvium. Particles are more angular than those in the modern Fulton Creek bedload, perhaps pointing to a nearby upvalley presence of Olympic valley ice. However, the fairly abundant organic fragments in the muddy facies seem less typical of a nearby ice front, which we would expect to have produced a sparsely vegetated, pebbly, cobbly braid plain characterized by rapid sedimentation and little woody debris.

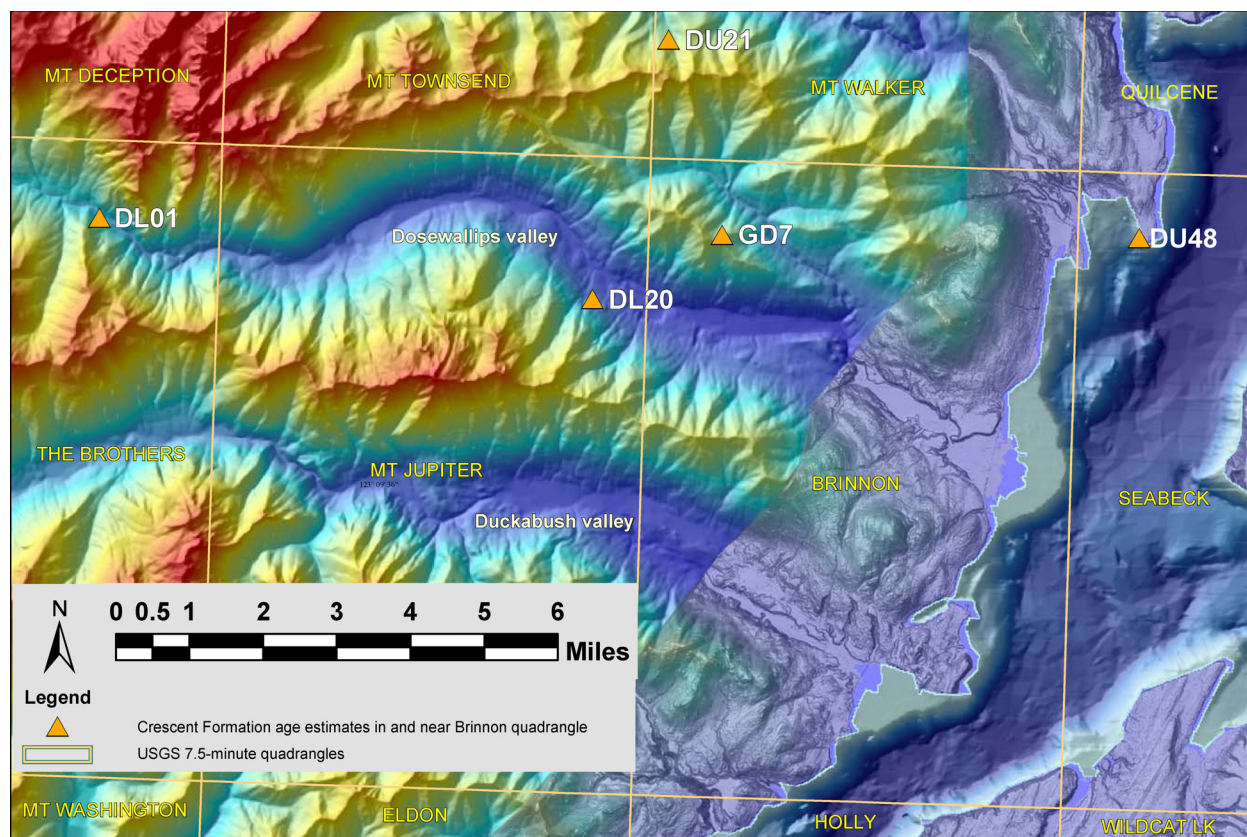


Figure A2. ^{40}Ar - ^{39}Ar date site locations from Crescent Formation volcanic rock samples in and near the Brinnon quadrangle. Dates from outside the Brinnon quadrangle are from Hirsch and Babcock (2009). Previously unpublished details for these age estimates (Table A1, for example, sample location coordinates) are courtesy Scott Babcock and David Hirsch (both Western Washington University; Scott Babcock, written commun., 2012).

Table A1. Age-control data from the map area and basalt ^{40}Ar - ^{39}Ar age estimates from a composite stratigraphic section of the Crescent Formation near the Dosewallips River (Hirsch and Babcock, 2009). Uncertainty values preceded by "±" are one standard deviation (68% confidence interval), and age ranges reported as "number-to-number" span two standard deviations ($2\sigma = 95\%$ confidence interval). Where the uncertainty value is in quotes, we do not know if it represents one or two standard deviations. Uncertainty statements reflect random and lab errors; errors from unrecognized sample characteristics or flawed methodological assumptions (for example, ^{14}C sample contamination from younger carbon flux or incomplete pre-depositional re-setting of luminescence samples) are not known. ^{14}C , radiocarbon analysis; AMS, radiocarbon analysis by accelerator mass spectrometry; OSL, optically stimulated luminescence analysis; IRSL, infrared stimulated luminescence analysis; ^{40}Ar - ^{39}Ar , Argon-40 to Argon-39-series analysis. See Figure A2 for sampled locations. One-sigma ^{14}C age estimates (including AMS) are in radiocarbon years before 1950 (^{14}C yr BP); ^{14}C ages stated in ka are in calendar years before 1950 divided by 1,000. One-sigma ^{14}C ages (including AMS) are "conventional" (adjusted for measured $^{13}\text{C}/^{12}\text{C}$ ratio). Geologic units are the interpretation of this study for the sample host material and, for subsurface samples, these may differ from map units. Altitudes are in feet (estimated using a USGS 10-meter digital elevation model derived from the topographic base map (whereon mean sea level (msl) = 0) and accessed via the Washington Department of Natural Resources GIS database or, where available, Puget Sound Lidar Consortium lidar grid altitudes projected to Washington State Plane South, NAD 83 HARN, U.S. Survey feet, supplemented by visual elevation estimates on bluffs). Lidar altitude statements were not adjusted to account for systematic projection differences relative to base map. Lidar level 0 theoretically is ~3 to 4 ft below base map level 0 (http://www.ngs.noaa.gov/cgi-bin/VERTCON/vert_con.pl). Latitude and longitude coordinates were generated from sample locations as plotted in ArcGIS (projection Washington State Plane South, NAD 83 HARN, U.S. Survey feet).

Date site	Site name	Lat/long (degrees)	Age estimate (^{14}C yr BP, ka, or Ma)	Analytic method	$^{13}\text{C}/^{12}\text{C}$ (o/oo)	Material dated	Map unit	Lab or lab no.	Alt. (ft)	Reference	Original sample ID	Notes
GD8	Duckabush landslide	47.66034 -122.93743	1,350 ±30 BP (1,300–1,260 ka)	AMS	-25.2	wood	Qls	Beta 315796	210	This report	11-09-M-0748	Western hemlock cones in landslide debris, exposed by stream channel wall. Organic debris positively identified as western hemlock (<i>Tsuga heterophylla</i>) by Rex Crawford, DNR Natural Heritage Program. We interpret the date as record of landslide movement about 1.3 to 1.26 ka (and saw no evidence of recent landslide movement). The slide developed in ice-contact deposits on fairly low slope angles (17–50%, based on three transects). Similar settings and ice-contact deposits around in the map area, similar slides do not, and the slide bears some morphologic similarity to the Alderwood landslide, suggested to be seismically induced, at the south end of Hood Canal (Polenz and others, 2009a). Within the limits of dating resolution, the 1.3 to 1.26 ka age is coeval with land level changes and landslide induced(?) valley damming in the Hamma Hamma basin (Contreras and others, 2012a), inviting speculation that this landslide may be seismically induced and linked to seismic effects in the Hamma Hamma basin (see "Structure" discussion in text).
GD9	Duckabush delta	47.64430 -122.92236	1,350 ±90 BP (1,410–1,070 ka)	^{14}C (with extended counting)	-29.2	wood	Qoam ¹	Beta 168714	Between -9.85 and -11.15	Lindstrum, 2002 and Emily Lindstrum written commun., 2012	DKSAUG 2001EL	Core sample from Duckabush River marine delta. ^{14}C sample extracted from "clay-rich mud" with "abundant" leaf fragments and mat-like organic material" collected from 70–71.5 cm downcore and interpreted by Lindstrum as tidal island soil from the uppermost intertidal range. Core surface altitude was reported at -2.3 m, thus yielding -9.9 ft sample depth. This is a minimum depth estimate because core recovery was incomplete, implying that true sample depth may be farther downsection. The sampled mud is in "sharp" contact with upsection and downsection "gravel" characterized as "well rounded, granule sized, clast supported, poorly sorted and matrix poor" and interpreted as river channel deposits. Lindstrum interpreted this and other Duckabush delta cores as a record of relative sea level rise, which she speculated was partly tectonic.
GD1	Dosewallips relict alluvium	47.70031 -122.91990	4,140 ±30 BP (4,820–4,570 and 4,560–4,550 and 4,540–4,530 ka)	AMS	-25.2	charred material	Qoa	Beta 315797	50	This report	11-92-R-033	Charcoal fragments from 2- to 3-ft-thick mud layer loaded with detrital charcoal, apparently a post-fire sediment pulse. Overlain by ~7 ft of planar bedded, apparently lacustrine mud. The date demonstrates a late Holocene origin for a relict alluvial terrace that is elevated ~15–20 ft above the active flood plain; unclear is why the valley floor from 4,500 years ago is so elevated. Possible explanations include a post-fire sediment pulse that provided enough sediment to temporarily elevate the valley floor, a down-valley landslide dam, tectonic base-level lowering, or late Holocene base-level lowering by bedrock incision at the basalt bedrock gorge 2,500 ft southeast of the sample site. The apparently lacustrine setting of the sample and upsection sediment favor a temporarily elevated base level, which could result from damming of the downvalley bedrock gorge. Although no landslide source area of obviously sufficient scale is apparent in the gorge walls, landslide damming appears to offer the simplest explanation for the valley floor aggradation.

Date site	Site name	Lat/long (degrees)	Age estimate (¹⁴ C yr BP, ka, or Ma)	Analytic method	¹³ C/ ¹² C (o/oo)	Material dated	Map unit	Lab or lab no.	Alt. (ft)	Reference	Original sample ID	Notes
GD3	Rocky Brook Vashon advance	47.74184 -122.97331	14,490 ±60 BP (17,820–17,530 ka)	AMS	-26.6	wood	Qga	Beta 315794	1,350	This report	11-25-M-0247A	Detrital wood in compact lake sediment. The lake was most likely impounded by Vashon Puget lobe ice approaching from down valley (entering Rocky Brook valley via the Dosewallips valley). The date is thus interpreted as marking the arrival about 17.8–17.5 ka of the Vashon Stade Puget lobe ice at 1,350 ft altitude in the map area.
GD4	Fulton Creek pre-Vashon	47.64401 -122.99844	19,600 ±80 BP (23,630–23,320 ka)	AMS	-24.1	wood	Qpuop	Beta 315795	1,000	This report	11-40-M-0418A	Detrital wood in pre-Vashon, Olympic-sourced, fluvio-lacustrine flood plain sediment (Fig. A1). Sample represents 23 mg composite of several small wood bits. It is unclear if setting is best interpreted as glacial or nonglacial.
GD2	Brinnon delta Vashon recessional	47.69940 -122.89742	21.7 ±2.50 ka 36.7 ±4.14 ka	OSL ² IRSL ⁴	— — —	sand	Qgol	11-82-M-0821	~90	This report ³	11-146-M-1206	Loose sand in late Vashon glaciolacustrine delta foreset beds. OSL: mean of 11 (of 25 attempted) replicated equivalent dose estimates; total dose rate 1.67 ±0.08 Gy/ka; equivalent dose 36.2 ±4.09 Gy. IRSL: total dose rate 2.29 ±0.11 Gy/ka; equivalent dose 84.1 ±4.54 Gy. Regional ¹⁴ C dates suggest more recent age (see also Table A2).
GD6	Black Point	47.65246 -122.90194	39.2 ±4.59 ka 40.2 ±2.46 ka	IRSL ⁴ OSL ²	— — —	sand	Qpu	11-82-M-0821	46	This report ³	11-82-M-0821	Fine sand 35 ft above beach in compact, lacustrine interbeds of sand, mud and pebbles, apparently from same lake deposit as at date site GD5 to south. Sample petrography and sparse to rare granitic clasts document a mix of northern-sourced sediment and Duckabush alluvium, suggesting association with a proglacial lake dammed by receding Cordilleran ice, seemingly incompatible with 40 ka age. IRSL: total dose rate 3.39 ±0.17 Gy/ka; equivalent dose 142 ±5.96 Gy. OSL: mean of 7 (of 19 attempted) replicated equivalent dose estimates; total dose rate 2.74 ±0.12 Gy/ka; equivalent dose 110 ±4.73 Gy.
GD5	Quatsap Point delta	47.64626 -122.90761	42.6 ±4.28 ka	IRSL ⁴	— — —	sand	Qpu	11-82-M-0820	11	This report ³	11-82-M-0820	Compact sand at beach top in glaciolacustrine delta foreset beds that extend from about 90 ft above sea level to beach (or below) and are truncated at top by lodgment till that is overlain by Vashon ice-contact deposits. Apparently from same lake deposit as at date site GD6 to north. Granitics were not seen at sample site but were noted at GD6 and along apparently same(?) unit farther north. Sample petrography and sparse to rare granitic clasts document a mix of northern-sourced sediment and Duckabush alluvium, suggesting association with a proglacial lake dammed by receding Cordilleran ice, seemingly incompatible with 40 ka age. Total dose rate 3.63 ±0.16 Gy/ka; equivalent dose 167 ±3.67 Gy.
GD7	Rocky Brook Crescent Formation	47.73538 -122.97868	36.76 ±0.32 Ma ⁵	⁴⁰ Ar– ³⁹ Ar	— — —	Basalt (flow)	Ev _c	11-19-M-0198	2730	This report	11-19-M-0198	Flow basalt from 13-ft-thick exposure; chemistry (Table B3) and location (Fig. A2) suggest association with lower third of upper Crescent Fm. Lab reports a plateau containing 70% of the ³⁹ Ar gas release and interprets the date as time of crystallization. Lab notes that three low-temperature heating steps indicate limited ⁴⁰ Ar loss due to a more recent event that did not affect the age estimate. For full analytical results of the ⁴⁰ Ar/ ³⁹ Ar analysis, contact the Washington Division of Geology and Earth Resources. The age estimate resembles a 36.18 ±0.23 Ma age estimate from a comparable(?) stratigraphic position near Lake Cushman, 24 mi southwest of this sample (Polenz and others, 2012b). Hirsch and Babcock (2009) reported an unexpectedly young (31.2 ±0.2 Ma) date for sample DL01 (see below) from the lower Crescent 8.5 mi east of this sample; reset paleomagnetism causes Babcock (written commun., 2012) to question the validity of that date.

Site name	Lat/long (degrees)	Age estimate	Analytic method	Material dated	Map unit	Lab or lab no.	Reference	Original sample ID	Notes
Crescent Formation age control data from outside the map area:									
Dosewallips section – Upper Crescent top	47.737 -122.857	50.5 ±1.6 ⁶ Ma ⁶	⁴⁰ Ar- ³⁹ Ar	basalt (flow)	Ev _c	Noble Gas Mass Spectrometry Lab, Oregon State University	Hirsch and Babcock (2009); Scott Babcock ⁷ and John Huard ⁷ , written commun., 2012	DU48	6-step plateau age on a fine-grained polygonal basalt flow, sampled at Pulali Point (see DU48 in ⁴⁰ Ar- ³⁹ Ar date locations map-Fig. A2); marks the top of the upper member of the Crescent Formation within the Dosewallips sequence (see Hirsch and Babcock, 2009, Fig. 2).
Dosewallips section – Upper Crescent base	47.773 -122.986	51.0 ±4.7 ⁶ Ma ⁶	⁴⁰ Ar- ³⁹ Ar	basalt (flow)	Ev _c	Noble Gas Mass Spectrometry Lab, Oregon State University	Hirsch and Babcock (2009); Scott Babcock ⁷ and John Huard ⁷ , written commun., 2012	DU21	1-step plateau age on fine-grained massive basalt flow, sampled in Tunnel Creek area (north slope Mt. Crag, see DU21 in ⁴⁰ Ar- ³⁹ Ar date locations map-Fig. A2); marks the top of the Crescent Formation upper member of the Dosewallips sequence (see Hirsch and Babcock, 2009, Fig. 2).
Dosewallips section – Lower Crescent top	47.721 -123.015	56.0 ±1.0 ⁶ Ma ⁶	⁴⁰ Ar- ³⁹ Ar	basalt (flow)	Ev _c	Noble Gas Mass Spectrometry Lab, Oregon State University	Hirsch and Babcock (2009); Scott Babcock ⁷ and John Huard ⁷ , written commun., 2012	DL20	5-step plateau age on a medium-grained massive basalt flow, Dosewallips River Road (see DL20 in ⁴⁰ Ar- ³⁹ Ar date locations map-Fig. A2), marks the top of the Crescent Formation lower member of the Dosewallips sequence (see Hirsch and Babcock, 2009, Fig. 2).
Dosewallips section – Lower Crescent base	47.734 -123.160	31.2 ±0.2 ⁶ Ma ⁶	⁴⁰ Ar- ³⁹ Ar	volcanic rock	Ev _c (?)	Noble Gas Mass Spectrometry Lab, Oregon State University	Hirsch and Babcock (2009); Scott Babcock ⁷ and John Huard ⁷ , written commun., 2012	DL01	Plateau age on a possibly post-Crescent, alkalic intrusive rock (as also present in Oregon Coast Range basalts, Parker and others, 2010). Sampled along Dosewallips River Road (see DL01 in ⁴⁰ Ar- ³⁹ Ar date locations map-Fig. A2) to mark base of lower member of Crescent Formation. Lab notes that Ar-spectrum is consistent with a legitimate age estimate. Babcock notes reset paleomagnetism and suggests the age may also be reset. The relatively young age estimate is joined by a 36.18 ±0.46 Ma age estimate from near Lake Cushman, 20 mi south of this sample (Polenz and others, 2012b) and the 36.76 ±0.32 Ma age reported above for date site GD7.

¹ Sample geologic unit differs from the map unit at the sample location because the sample was collected offshore (where the base map shows water, sample GD9).

² Dose rate and age for fine (180–90 microns) quartz sand. Linear + exponential fit used on equivalent dose, with single aliquot regeneration. Errors to one σ .

³ Analysis by Shannon Mahan, U.S. Geological Survey, 2012.

⁴ Analysis performed on K-spar grains from polymineral fine silt fraction (5–10 microns) by multiple aliquot additive dose technique and using exponential fit for equivalent dose. Errors to one σ . Fade tests indicate no correction.

⁵ Analysis by Noble Gas Mass Spectrometry Lab, College of Earth, Ocean, and Atmospheric Sciences, Oregon State University, Corvallis. Lab analyzed ~70 mg of sample, irradiated 6 hours at 1 MW power at Oregon State University TRIGA reactor, April 30, 2012. Methods otherwise similar to those described by Koppers and others (2003). Lab used FCT-3 biotite known 28.03 ±0.18 Ma age standard (Renne and others, 1994).

⁶ Analysis by Noble Gas Mass Spectrometry Lab, College of Earth, Ocean, and Atmospheric Sciences, Oregon State University, Corvallis. Lab cautions that it is unclear if the analyses were reported as 1σ or 2σ , although it was probably 2-sigma (John Huard, written commun., 2012) and suggests they are less reliable than more recent analyses because they were performed in 1991 using old equipment (MS-10 mass spectrometer designed in the 1950s-1960s).

⁷ Scott Babcock: Western Washington University. John Huard: Noble Gas Mass Spectrometry Lab, College of Earth, Ocean, and Atmospheric Sciences, Oregon State University, Corvallis.

Table A2. Infrared stimulated luminescence (IRSL) and optically stimulated (OSL) data and age estimates compared to ages suggested by regional radiocarbon data. The (poorly constrained) luminescence age estimates for the Vashon recessional Brinnon delta suggest older deposits than would be anticipated from the regional radiocarbon data. If the age estimates for Quatsap and Black Points are systematically offset as much as those from the Brinnon delta (see column on luminescence-based age / ^{14}C -based age), this suggests a possible Vashon advance age for the Quatsap point delta deposit.

Site name	Sample information	Water content (%) ^a	K (%) ^b	U (ppm) ^b	Th (ppm) ^b	Cosmic dose additions (Gy/ka) ^c	Total dose rate (Gy/ka)	Equivalent dose (Gy)	n ^d	Age estimate (ka)	Time (ka) of sample deposition suggested by ^{14}C data	Ratio of luminescence-based age / ^{14}C -based age
Brinnon delta (GD2)	11-146-M-1206, Brinnon quad, Dosewallips valley	6 (16)	1.06 ±0.05	0.95 ±0.11	4.01 ±0.33	0.17 ±0.02	1.67 ±0.08	36.2 ±4.09	11 (25)	21.7 ±2.50 ^e	16.0 ^g	1.36
Quatsap Point delta (GD5)	11-82-M-0820, Brinnon quad, Hood Canal	5 (26)	1.76 ±0.06	1.91 ±0.14	8.46 ±0.61	0.03 ±0.01	2.29 ±0.11 ^f	84.1 ±4.54 ^f	—	36.7 ±4.14 ^f	16.0 ^g	2.29
Black Point lakebeds (GD6)	11-82-M-0821, Brinnon quad, Hood Canal	7 (31)	1.89 ±0.06	2.11 ±0.13	9.27 ±0.66	0.14 ±0.01	2.74 ±0.12	110 ±4.73	7 (19)	40.2 ±2.46 ^e	17.5 ^h	2.43
							3.39 ±0.17 ^f	142 ±5.96 ^f	—	39.2 ±4.59 ^f	17.5 ^h	2.24

^a Field moisture, with figures in parentheses indicating the complete sample saturation %. Ages calculated using approximately 60% of saturation values.

^b Analyses obtained using laboratory Gamma Spectrometry (high-resolution Ge detector).

^c Cosmic doses and attenuation with depth were calculated using the methods of Prescott and Hutton (1994). See text for details.

^d Number of replicated equivalent dose (De) estimates used to calculate the mean. Figures in parentheses indicate total number of measurements made, including failed runs with unusable data.

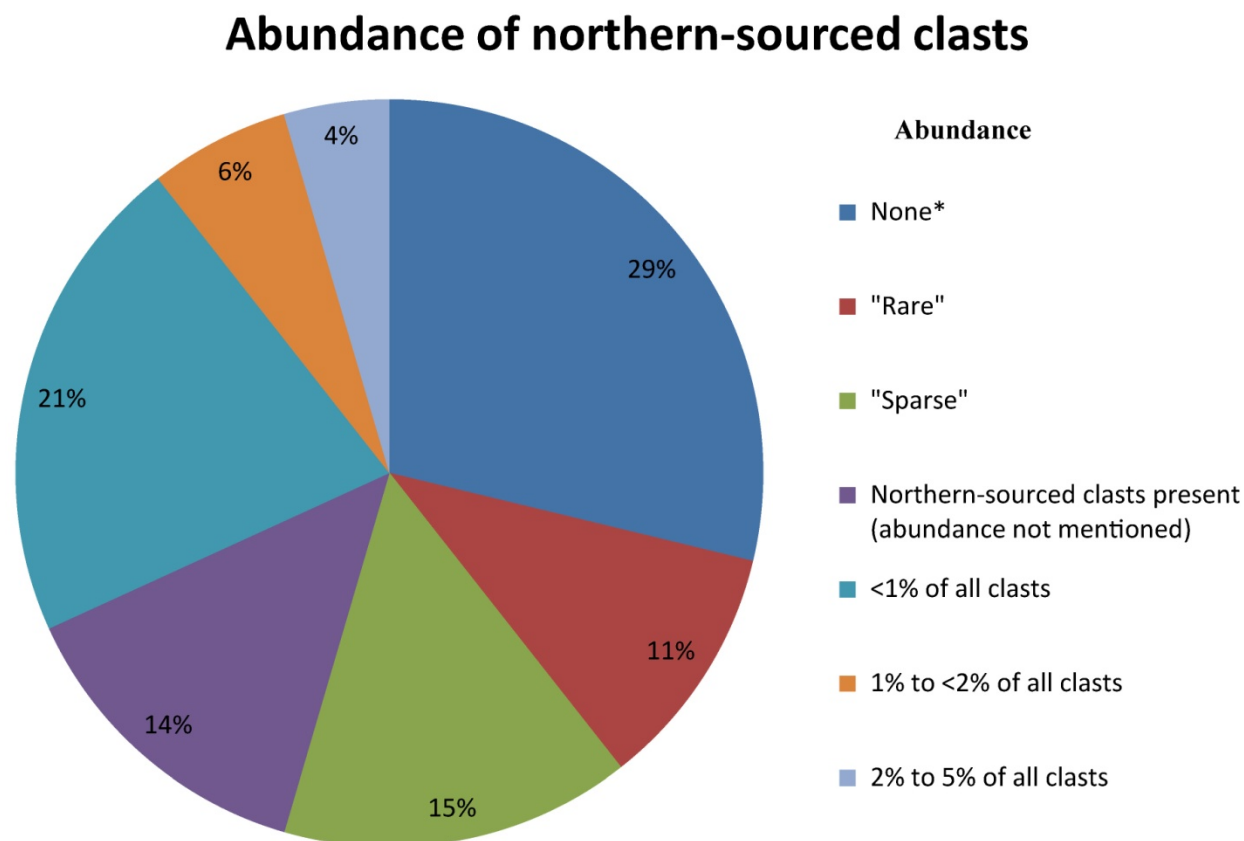
^e OSL age estimates: Dose rate and age for fine (180-90 microns) quartz sand. Linear + exponential fit used on equivalent dose, with single aliquot regeneration. Errors to one σ .

^f IRSL age estimates: Feldspar from fine grains of 4-11 micron polymineral silt. Exponential fit used for equivalent dose, multiple aliquot additive dose. Errors to one σ . Fade tests indicate no correction.

^g Rationale: Abundant stagnant ice deposits and the absence of a succession of terminal moraines on the Kitsap Peninsula suggest that the Vashon ice sheet in the western Puget Lowland disintegrated all at once across the entire Kitsap Peninsula (Haugerud, 2009, discussion on latest Pleistocene deglaciation in preliminary geomorphic map of the Kitsap Peninsula). Porter and Swanson (1998) called on four radiocarbon dates from Seattle and Lake Carpenter (near Kingston, northern Kitsap Peninsula) to assert that those areas were post-glacially ice free by about 16,000 calendar years ago, suggesting a rapid retreat (although it is not necessarily clear that conditions in the central Puget Lowland fully corresponded to coeval conditions at Hood Canal). Thus radiocarbon data suggest that 16,000 years ago is a reasonable time point estimate for Brinnon delta deposition.

^h Rationale: The Quatsap Point delta and Black Point lakebeds yielded indistinguishable luminescence age estimates, thereby strengthening the field-based suspicion that the delta and lakebeds are coeval facies within the same lake system. The same age is therefore assumed for both. A new radiocarbon date from Vashon advance glaciolacustrine sediment along Rocky Brook (age date site GD3, altitude 1,350 ft, 4 mi upvalley of the Dosewallips valley mouth; Table A1) suggests that Vashon Slade ice had arrived and impounded a proglacial lake to a valley elevation of 1,350 ft by 17,800 to 17,500 calendar years ago. Olympic-sourced ice could alternatively have impounded this lake. The dam was downvalley of the sample site, suggesting that the ice moved upvalley from the Rocky Brook-Dosewallips River confluence. There is little reason to expect Olympic ice to have invaded Rocky Brook in this manner unless faced by Vashon Puget lobe ice. If Olympic ice in the Dosewallips valley had, in the absence of Puget lobe ice, risen to sufficient thickness to inundate Rocky Brook to 1,350 ft altitude, it seems likely that Rocky Brook valley itself would have been glaciated from upvalley. This suggests that the date is associated with the arrival of Vashon Puget lobe ice in the area. Furthermore, three 14C dates from the Hoodport and Skokomish Valley and Union quadrangles (south of the Brinnon quadrangle) suggest that the Vashon ice arrival (ice advance) there took place between 17,000 and 15,300 calendar years ago (Polenz and others 2012b). Thus radiocarbon data suggest that Puget lobe ice had reached a thickness of 1,350 ft at the latitude of the Dosewallips River by 17,500 years ago, and if a proglacial lake were impounded at the ice front, that lake would have risen to the topset-foreset contact altitude (unknown due to truncation of forest beds by till at top, but >90 ft above modern sea level) at the Quatsap Point delta somewhat earlier. A radiocarbon-based age estimate of 17,500 years thus conservatively estimates the time of formation of the Quatsap Point delta if the delta is assumed to have formed in a Vashon advance proglacial lake.

Appendix B. Lithologic and Petrographic Trends Among Sediments



* Estimates number of sites where no granitic clasts were identified. Number of sites that actually lacked granitic clasts likely is smaller because some site reviews were not exhaustive.

Figure B1. A review and comparison of field sites in which abundance of northern-provenance clasts was mentioned. Field notes from 66 northern-sourced drift observation field sites west of, but close to, the shore of Hood Canal were reviewed for their mention of northern-provenance clasts. Pebble counts in northern-sourced drift at two sites east of Hood Canal revealed that east of Hood Canal, diagnostically northern-sourced clasts constitute at least 15 percent of all clasts, and granitic clasts 1 to 6 percent. West of Hood Canal, we noted less than 5 percent granitic clasts at all 66 drift observation sites, and less than 1 percent at 40 (70%) of the 57 sites for which we estimated the percentage of granitic clasts. West of Hood Canal we also failed to note any granitic clasts in 19 (33%) of 66 sites for which we noted whether granitic clasts were observed (including some sites where we did not estimate percentages).

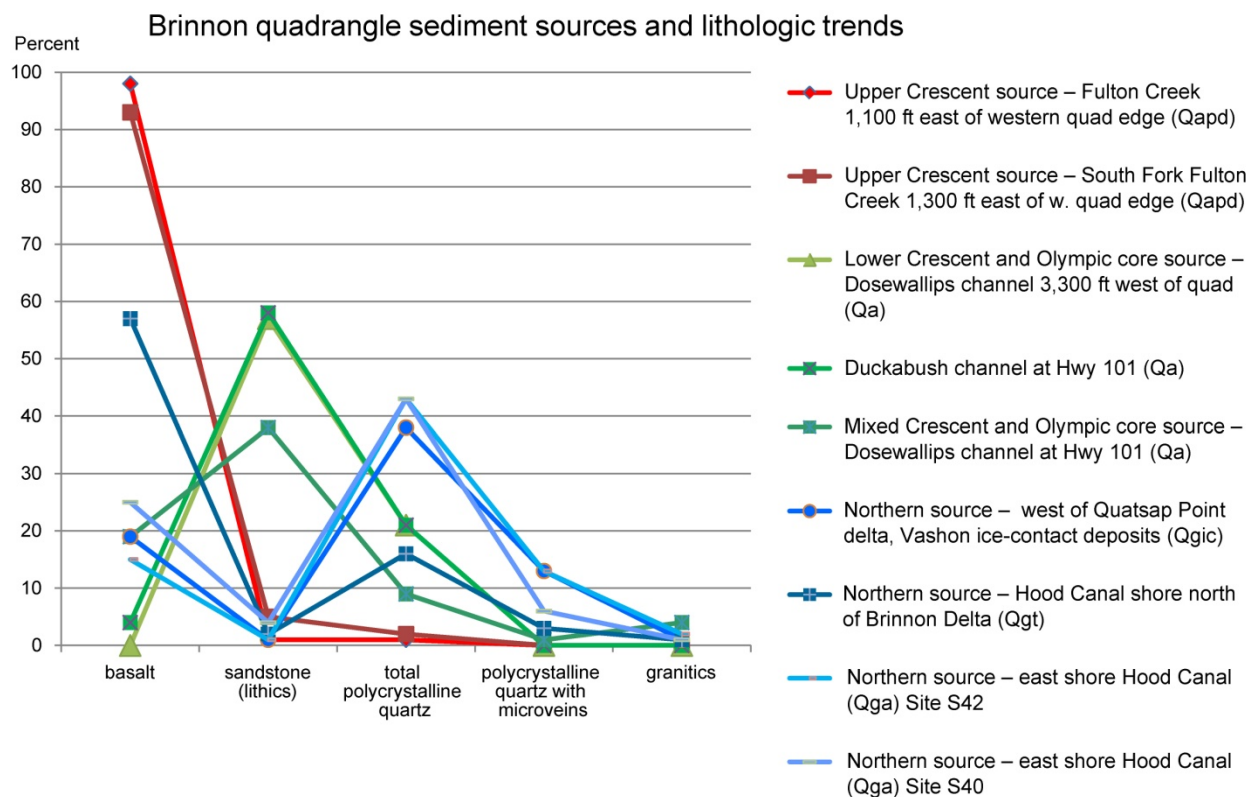


Figure B2. Graph of lithologic properties vs. abundance (%) in sand based on sediment source. The graph illustrates that the least ambiguous indicator of a northern source is polycrystalline quartz with microveining—any northern-sourced sample contained more of it than any Olympic-sourced sample. The Olympic-sourced samples contain 0 to 1 percent polycrystalline quartz with microveining, and samples from the lower Crescent Formation and Olympic core rocks have a high content (>38%) of lithic fragments, whereas upper Crescent Formation samples contain >90 percent basalt. (See also Table B1.)

Table B1. Lithologic and petrographic trends in thin sections of sand from Olympic- vs. northern-sourced samples. Thin sections of Olympic-sourced sediment samples for which the source area is upper Crescent Formation consist of more than 90 percent basalt, whereas thin sections of samples from deposits that include sediment derived from areas mapped as lower Crescent Formation or Olympic core rocks include 38 to 58 percent lithic fragments and 9 to 21 percent polycrystalline quartz (but never more than 1 percent with microveining). Thin sections also revealed that modern Dosewallips and Duckabush River alluvium contained less than 20 percent basalt and more than 35 percent lithic fragments, whereas drift samples of exclusively upper Crescent derivation and northern-sourced samples contained at most 5 percent lithic fragments. Thin sections of northern provenance samples from west of Hood Canal contained 16 to 38 percent polycrystalline quartz, including 3 to 13 percent with microveining. In thin sections of samples from east of Hood Canal, we found more than 40 percent polycrystalline quartz, including 6 to 13 percent with microveining.

	Sample site ID	% basalt	% lithics	% total polycrystalline quartz	% Polycrystalline quartz with quartz microveins	% granitic clasts	Sample source
upper Crescent Formation	S39	98	1	1	0	0	Upper Crescent Formation source – Fulton Creek 1,100 ft east of western quad edge (Qapd)
	S41	93	5	2	0	0	Upper Crescent Formation source – South Fork Fulton Creek 1,300 ft east of western quad edge (Qapd)
lower Crescent Formation and core rocks (Dosewallips Channel)	11-92-M-0925	<1	57	21	0	0	Lower Crescent Formation and Olympic core source – Dosewallips channel 3,300 ft west of quad (Qa)
upper and lower Crescent Formation and core rocks (Duckabush and Dosewallips Channels at US101)	S37	4	58	21	<1	0	Mixed Crescent Formation and Olympic core source – Duckabush channel at Hwy 101 (Qa)
	S36	19	38	9	1	4	Mixed Crescent Formation and Olympic core source – Dosewallips channel at Hwy 101 (Qa)
Hood Canal west shore	S38	19	1	38	13	1	Northern source – west of Quatsap Point delta, Vashon ice contact deposits (Qgic). Granitic clasts readily apparent in outcrop. A few are rotten. Some may have been interpreted as pre-Vashon by Frisken (1965) and Bretz (1913).
	S35	57	2	16	3	1	Northern source – Hood Canal shore north of Brinnon delta (Qgt)
Hood Canal east shore (Kitsap Peninsula)	S42	15	1	43	13	2	Northern source – east shore Hood Canal (Qga). Some polycrystalline quartz looks metamorphosed, as in quartzite. Field estimate: among 48 clasts (broken on site) at least 15% to 30% were northern-sourced clasts. This includes at least 6% granitic clasts. (Note the much lower northern-sourced content recognized in thin section.)
	S40	25	4	43	6	1	Northern source – east shore Hood Canal (Qga)

Appendix C. Relict Lakeshore Levels

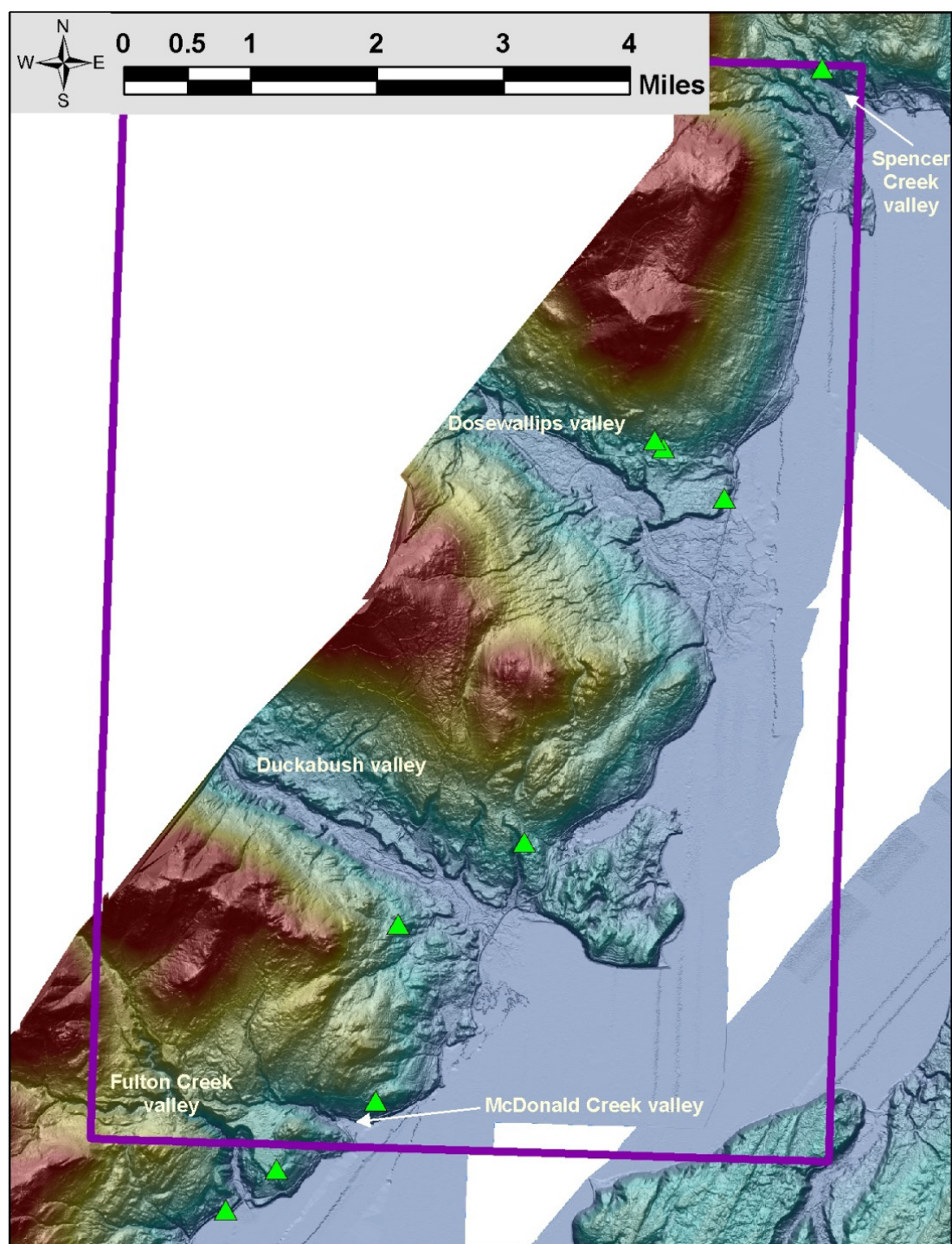


Figure C1. Lidar shaded-relief image with relict lake shore level data points in and near the Brinnon quadrangle (purple rectangle). Green triangles mark data points from Table C1 and Figure C2 (plot of lake shore level indicators). Image is a composite of vertical and 45 degrees northern sun angles and has six times vertical exaggeration. Image color serves as a proxy for altitude; relief above 1000 ft is red and below 300 ft is greenish blue to blue.

Table C1. Elevations of relict lake delta tops and other shoreline markers from Vashon glaciorecessional, ice-dammed lakes along the west shore of central and southern Hood Canal. Lake-shore markers from the Skokomish Valley and Hoodsport quadrangles along southern Hood Canal are from Polenz and others (2012b) with added latitude and longitude coordinates. Polenz and others (2012b) observed only a single lakeshore marker at any one latitude and inferred that all their observed shores probably represent the same lake, despite notable scatter in the altitude data set (blue squares in Fig. C2). Assuming that a given set of shores was formed by the same lake, differences among lake shore elevations reveal land-level changes that followed the Vashon Stade incursion of Cordilleran ice into the Puget Lowland. Thorson (1989) interpreted such regional changes as a measure of north-up earth surface tilting associated with glacio-isostatic crustal rebound. He quantified the tilt angle at 1m/km, represented by the lilac "regional rebound slope" line in Fig. C2. The Y-axis intercept of the line at 240 ft represents the modern altitude of the putative lake drain at Purdy Canyon (Polenz and others, 2010a) and consequently suggests lakeshore altitudes expected farther north. Polenz and others (2012b) offered multiple scenarios to explain the scatter in their dataset and noted that the similarity between Thorson's regional tilt and the slope angle of a best-fit line through their dataset (blue line in Fig. C2) may be coincidental, especially in light of the discrepancy of the Y-axis intercepts. The Brinnon dataset clearly includes a record of at least two lake levels (green data points in Fig. C2; Brinnon area site locations are shown in Fig. C1 and include two data points from the Holly quadrangle just south of the Brinnon quadrangle). Additional evidence for the more recent, lower lake level is partly illustrated by Figure C3, but was not added to the table and Figure C2 because a brief survey indicated that the lower lake features reasonably parallel those of the upper data set. The slopes of the best fit lines for the two lake levels do not differ much from each other and approximate Thorson's regional rebound tilt angle. Multiple flights of benches can in some places be identified near (mostly slightly below) the upper lake level along the northern flanks of both the Duckabush and Dosewallips River valleys. The magnitude of bench level ranges is illustrated by the isolated data point at 322 ft, which was excluded from the Brinnon area rebound slope trend line. Because such multiple bench sets were recognized only on the northern valley sides of both major drainages, we suspect that they are associated with kame terracing rather than multiple lake levels. A tectonic explanation (with structural offset across each of the two valleys) seems unlikely in light of the minimal scatter in the overall record of the upper lake. See "Ice-dammed Vashon recessional lakes" and "Structure" for discussion and possible tectonic significance of the lake-level data.

Quad	Site location	Altitude (ft)	Distance (mi) from Purdy Canyon outwash	Elev. change (ft) to Purdy Canyon	Slope (ft/mi) to Purdy Canyon	Latitude	Longitude
Skok Valley	Purdy Canyon, lowest outwash terrace (Polenz and others, 2010a)	240	0	0	n.a.	47.29553	-123.17994
Skok. Valley	South of Potlatch State Park (bench, interpreted as beach)	220	4.6	-20	-4.348	47.36135	-123.16336
Skok. Valley	South of Potlatch Hydropower standpipe (bench, interpreted as beach)	225	5.1	-15	-2.941	47.36864	-123.16303
Skok. Valley	North of Potlatch Hydropower standpipe (bench, interpreted as beach)	232	5.4	-8	-1.481	47.37265	-123.16298
Hoodsport	Northern Potlatch south (delta and bench, interpreted as beach)	250	6.1	10	1.639	47.38243	-123.15385
Hoodsport	Northern Potlatch north 1 (bench, interpreted as beach)	250	6.5	10	1.538	47.38743	-123.15041
Hoodsport	Northern Potlatch north 2 (bench, interpreted as beach)	250	7	10	1.429	47.39493	-123.15035
Hoodsport	South of Finch Creek (bench, interpreted as beach)	241	7.6	1	0.132	47.40359	-123.15566
Hoodsport	South of Miller Creek (delta)	248	9.4	8	0.851	47.42682	-123.13050
Holly	South of Fulton Creek (bench, interpreted as delta)	96	24.16	-144	-5.960	47.61723	-122.97797
Holly	North of Fulton Creek (bench, interpreted as delta)	314	24.6	74	3.008	47.62206	-122.96956
Brinnon	North of McDonald Creek (bench, interpreted as beach)	320	25.4	80	3.150	47.63016	-122.95310
Brinnon	South of Duckabush River (bench, interpreted as beach or kame terrace near lakeshore)	333	26.8	93	3.470	47.65037	-122.95022
Brinnon	Bench north of Duckabush River (marks base of channel; interpreted as delta)	337	27.8	97	3.489	47.66022	-122.92931
Brinnon	Brinnon delta (delta for lower lake, and therefore excluded from trendline)	135	30.9	-105	-3.398	47.70015	-122.89722
Brinnon	Upper shoreline(s)? above Brinnon delta, lower bound (excluded from trendline)	322	31.1	82	2.637	47.70562	-122.90774
Brinnon	Upper shoreline(s)? above Brinnon delta, upper bound (bench, interpreted as beach)	357	31.1	117	3.762	47.70648	-122.90932
Brinnon	Spencer Creek outwash terrace (likely delta top) (bench, interpreted as beach)	380	34.3	140	4.082	47.749	-122.883
	Slope yielded by 0.06° regional rebound tilt estimate of Thorson (1989)	428	34	188	5.529	47.617	-122.978

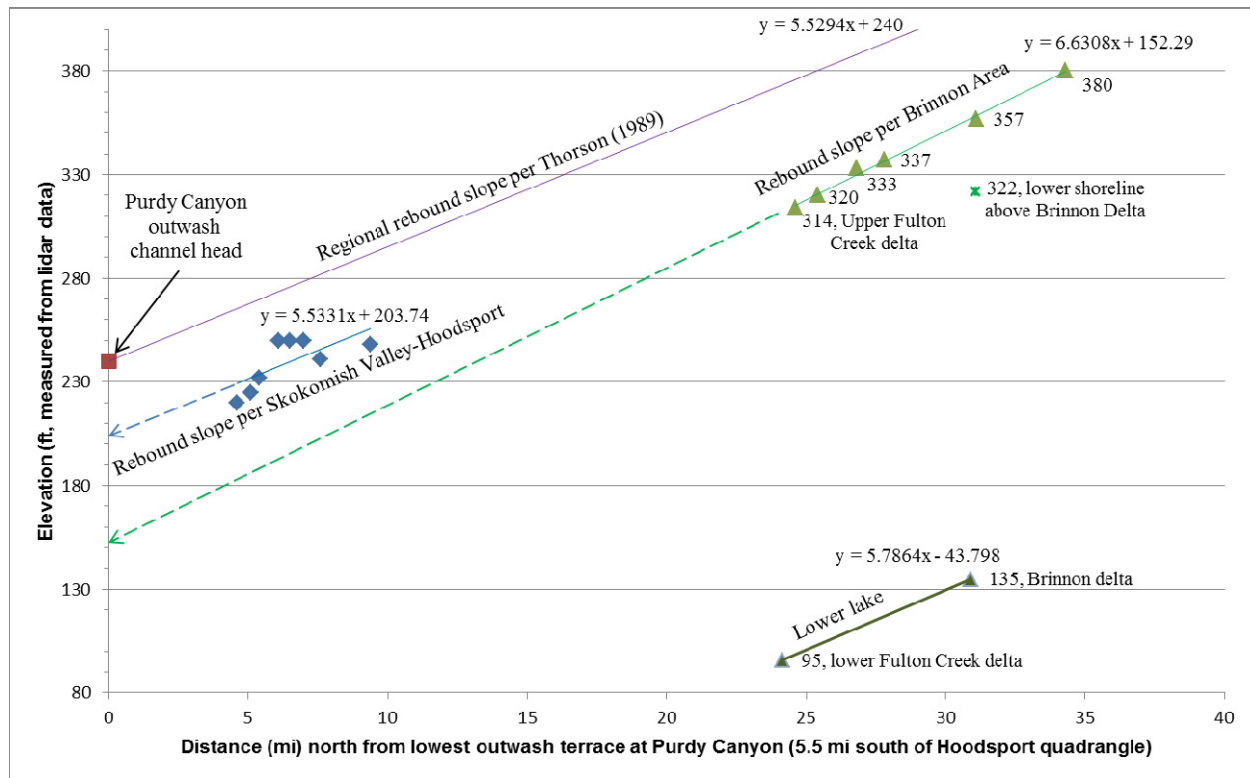


Figure C2. Relict lake shore altitude markers and implied post-glacial land level changes and tilt slope angles along central and southern Hood Canal.

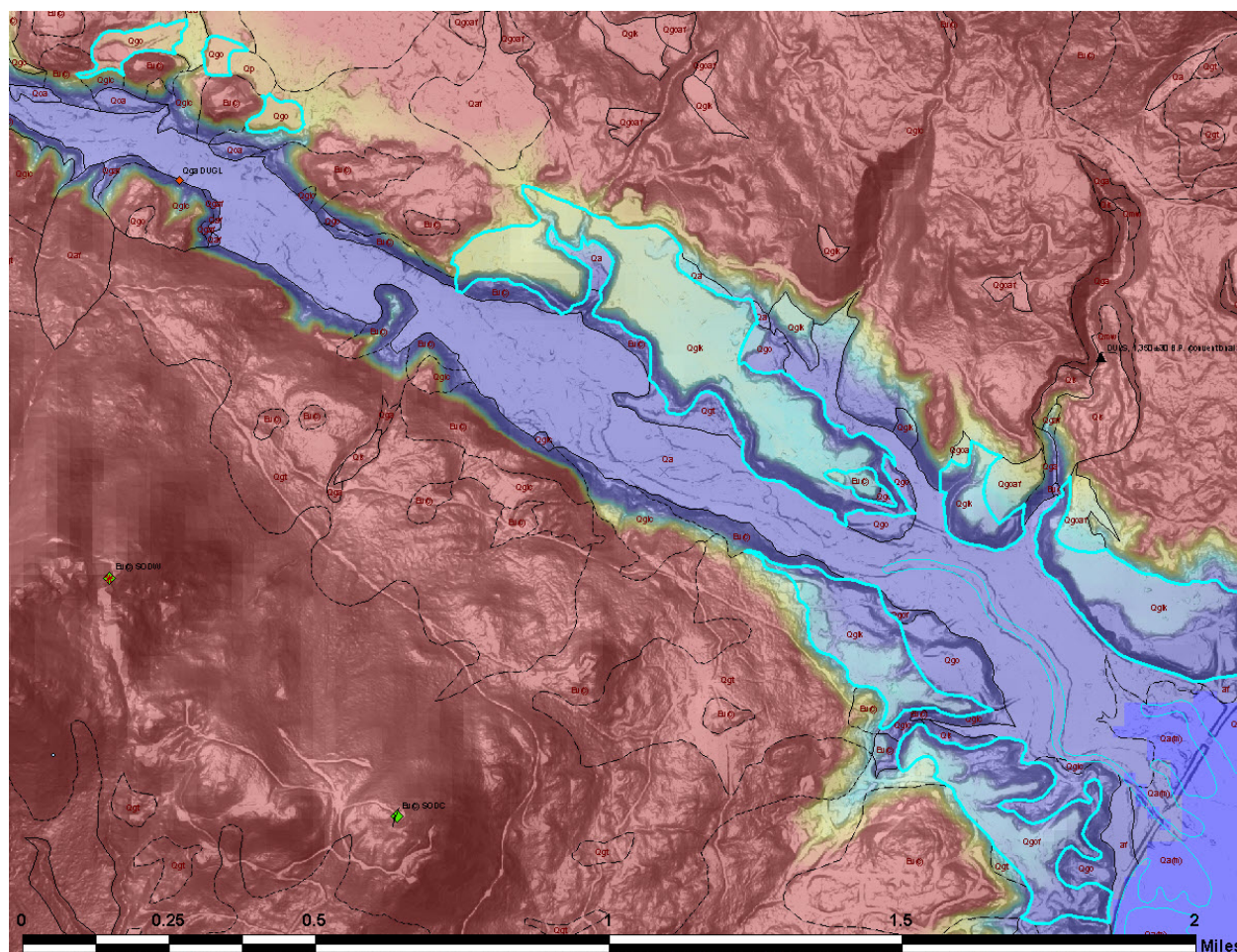


Figure C3. Lower Duckabush River valley lidar hillshade image with vertical, simulated sun angle. Blue indicates altitude below 100 ft, red above 165 ft. Large, relict terraces (blue to yellow, outlined by pale blue lines) along both sides of the lower Duckabush River valley smoothly rise northwestward from about 100 ft (near marine shore in lower right of image) to about 160 ft (upper left of image). The 60-ft rise over 2 mi contrasts with a 45-ft elevation gain for the modern Duckabush channel along the same valley reach. The 33 percent steeper relict terrace slope is consistent with the higher sedimentation rate expected of a glaciorecessional environment. Exposures in the southernmost terraces in the lower right of the image document that some deposits near the valley mouth are lacustrine (unit Qgof). Their altitude of about 100 ft near the valley mouth suggests that the terraces were graded to the same lake as the Brinnon delta to the north and the lower Fulton Creek delta to the south. (See “Ice-dammed Vashon recessional lakes”, Table C1, and Figs. C1 and C2.)

Appendix D. Selected Structural Data: Seismicity, Faults, and Joints

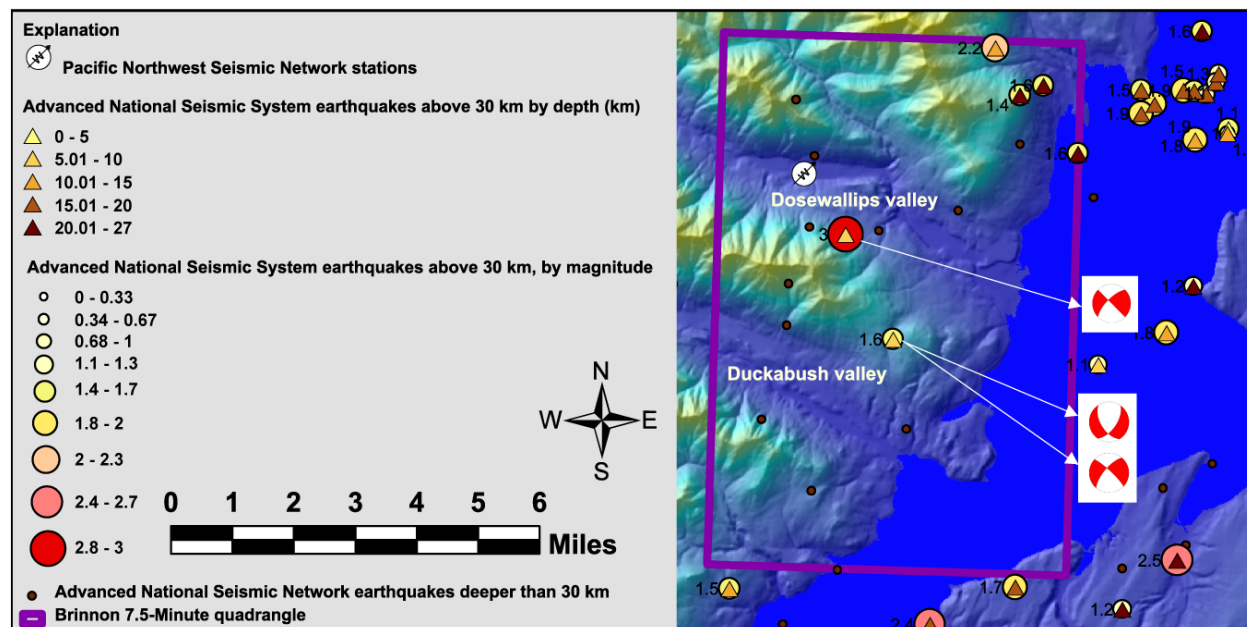


Figure D1. Known earthquake catalog information (1970–2011, <http://www.quake.geo.berkeley.edu/anss/catalog-search.html>), showing earthquake locations, depths, and magnitudes in and near the Brinnon quadrangle. Most known earthquake hypocenters in the quadrangle are more than 30 km beneath the surface (small brown dots) and are interpreted as Benioff zone events associated with the descent of subducting seafloor. Tom Yelin and PNSN.org (written commun., 2012, and ftp://ftp.geophys.washington.edu/pub/seis_net/focal.AMcards; for explanations, see ftp://ftp.geophys.washington.edu/pub/seis_net/focal.readme and <http://www.pnsn.org/outreach/faq/focal-mechanisms>) provided analyses of focal mechanisms from crustal earthquakes within the quadrangle. We felt that two earthquakes yielded presentable focal mechanism solutions. Both were strike-slip events. The larger (Mc 3.0) occurred about 9 km below the surface and is marked by the larger red dot and has a single fault mechanism solutions diagram (“beach ball” in center of right quadrangle margin). The smaller (Mc 1.6) occurred about 7 km below the surface and is marked by the yellow dot (southwest of the larger). It has two competing possible fault mechanism solutions diagrams (lower right margin), one of which closely resembles the solutions diagram for the Mc 3.0 event. Neither earthquake is located along a known fault, and we do not have enough earthquake data and corresponding surface observations to clearly favor one fault orientation, but we note that right-lateral offset could place both earthquakes on a single postulated fault (not shown), and we observed evidence of strike slip in a fault near the northwest corner of the map (map and Fig. D2). This observed fault is approximately on trend with a line between the two earthquakes. (We thought chatter along the slickensides favored right-lateral motion.) However, we do not have an explanation for how such a structure would fit into regional tectonic trends.



Figure D2. Subvertical fault exposed south of Rocky Brook in a cutbank along Forest Road 2630 (sec. 13, T26N R3W; N. 47.74507°; W. 122.99653°). The fault strikes 150 to 160 degrees (SSE) and is flanked to the west by a fault-parallel fracture set and to the east by a 15-ft-wide zone of broken rock. Faint slickensides in multiple orientations suggest strike-slip. Chattermarks on the slickensides appear to favor right-lateral slip with a northeast-down component. Because we were unable to trace the fault beyond one outcrop and lack information regarding activity, we show it only as short (1000-ft-long) segment, coded as inferred and queried at both ends. Speculative association with known earthquakes is discussed in the caption for Figure D1.



Figure D3. Joint control on Fulton Creek channel walls and waterfall surfaces at significant site S33. The dominant joint set is near-vertical and trends close to east-west. Upper image: view west (upvalley); the channel walls are joint controlled, and joints in the northern wall (image right, see arrows) are especially prominent at 104-83 (average of three measurements: 104-74; 105-82; 104-93). The same joint set also forms the planar faces of several waterfalls on an 80-ft-tall knickpoint in the channel (low end of falls visible in image center). Lower image: view east (downvalley) of the same joint orientation (see arrow) that forms the northern channel wall to the left of Logan Fusso.

Appendix E. Geochemical Data

Table E1. X-ray fluorescence (XRF) and loss on ignition (LOI) analyses for an andesite pebble sampled at ~70 ft altitude in a deltaic foreset sand bed at geochemistry site G1, about 900 ft north of Quatsap Point, Brinnon quadrangle. The deltaic beds are exposed between 0 (beach substrate) and ~90 ft (where foreset beds are truncated by upsection till). Elevation within that range is not meaningful, but exposures of volcanic pebbles like the one analyzed here are rare and were observed only in the stratigraphically upper half of the exposures of unit Qpu north and southwest of Quatsap Point. Analyses (XRF and LOI) performed by the Washington State University Geoanalytical Laboratory (Pullman, Wash.), March 2012.

SiO ₂	61.09	SiO ₂	62.80
TiO ₂	0.518	TiO ₂	0.532
Al ₂ O ₃	18.02	Al ₂ O ₃	18.53
FeO	4.28	FeO	4.40
MnO	0.090	MnO	0.092
MgO	2.60	MgO	2.68
CaO	5.12	CaO	5.27
Na ₂ O	4.18	Na ₂ O	4.30
K ₂ O	1.09	K ₂ O	1.12
P ₂ O ₅	0.272	P ₂ O ₅	0.280
Sum	97.28	Total	100.00
LOI (%)	2.46		
Unnormalized Trace Elements (ppm):		Major elements are normalized on a volatile-free basis, with total Fe expressed as FeO.	
Ni	45	NiO	56.9
Cr	37	Cr ₂ O ₃	53.5
Sc	12	Sc ₂ O ₃	17.7
V	83	V ₂ O ₃	121.6
Ba	619	BaO	691.5
Rb	14	Rb ₂ O	15.8
Sr	825	SrO	975.1
Zr	111	ZrO ₂	FALSE
Y	15	Y ₂ O ₃	19.3
Nb	4.3	Nb ₂ O ₅	6.1
Ga	20	Ga ₂ O ₃	26.9
Cu	23	CuO	28.6
Zn	62	ZnO	77.5
Pb	7	PbO	8.0
La	13	La ₂ O ₃	14.8
Ce	23	CeO ₂	28.1
Th	3	ThO ₂	3.2
Nd	13	Nd ₂ O ₃	15.2
U	1	U ₂ O ₃	1.2
		Cs ₂ O	0.0
		As ₂ O ₅	0.0
		W ₂ O ₃	0.0
sum tr.	1930	sum tr.	2161
in %	0.19	in %	0.22
sum m+tr	97.47		
M+Toxides	97.49		
w/LOI	99.95		
if Fe3+	100.42		

Table E2. Comparison of X-ray fluorescence (XRF) analytical results for a Cascades-sourced volcanic pebble (sample 11-81-M-0783) sampled within the Quatsap Point delta (significant site G1; see also Table E1) and XRF and inductively coupled plasma mass spectrometry (ICP-MS) results for 107 Glacier Peak volcanic clasts (Dragovich and others, 2005) and four volcanic clasts from apparent Possession Drift of unit Qvc from Tekiu Point Road and Thunder Ridge Way in the Holly 7.5' quadrangle (south of the Brinnon quadrangle, Contreras and others, 2012b). Polenz and others (2005) interpreted similarity of the average of 20 clasts from Whidbey Island to the 107 Glacier Peak clasts as evidence of a Glacier Peak origin of lahars run-out deposits on Whidbey Island. Contreras and others (2012b) interpreted their four clasts as a probable Glacier Peak-sourced deposit based on an electron microprobe analysis of sample 2-K-9B (Thunder Ridge Way) and the similarity of their XRF data to those from known Glacier Peak-sourced deposits. The XRF data below suggest that among the five Hood Canal area samples analyzed to date, sample 2-K-9B is the most similar to Glacier Peak and the Quatsap Point sample the least. Where Hood Canal area samples revealed an oxide content more than two standard deviations away from the mean of 107 Glacier Peak-sourced samples, the columns on the right identify the oxide in question with entries of "too high" (sample contained this oxide in excess of Glacier Peak average plus 2σ) or "too low" (sample contained less of this oxide than Glacier Peak average minus 2σ). Geochemically noteworthy differences between the Quatsap Point pebble and those from Tekiu Point and Thunder Ridge Way include a lower K₂O value and a higher Na/K ratio for the Quatsap Point pebble. The differences of all Hood Canal samples relative to Glacier Peak data do not rule out a Glacier Peak origin but suggest that volcanic sources in Canada and small intrusive centers west of the main Cascade volcanic arc merit consideration, in part because at least the Quatsap Point sample is weakly adakitic (Michael Glynn, USGS, written commun. 2012). No such fitting source has been identified to date.

Sample ID	(11-81-M-0783)	53S179A	1-T-13	2-K-9-Bb	K-9-B	Ave. of 20 Whidbey Is. volcanic clasts (Polenz and others, 2005)	Standard deviation of 20 clasts (Polenz and others, 2005)	Ave. of 107 Glacier Peak dacite clasts from east/north of Whidbey Is. (Dragovich and others, 2005)	Standard deviation of 107 clasts (Dragovich and others, 2005)	Low bound: Glacier Peak average of 107 - 2 standard deviations	High bound: Glacier Peak average of 107 + 2 standard deviations	Is Quatsap Point pebble outside 2 standard deviation range for Glacier Peak source?	Is Tekiu Point Rd NW pebble (53S179A) outside 2 standard deviation range for Glacier Peak source?	Is Tekiu Point Rd NW pebble (1-T-13) outside 2 standard deviation range for Glacier Peak source?	Is Thunder Ridge Way pebble (2-K-9-Bb) outside 2 standard deviation range for Glacier Peak source?	Is Thunder Ridge Way pebble (K-9-B) outside 2 standard deviation range for Glacier Peak source?	
Latitude	47.649	47.57945	47.57935	47.5854	47.5854	65.6	0.88	65.09	1.24	62.6	67.6	---	---	---	---	---	SiO ₂
Longitude	-122.906	-122.959	-122.96	-122.951	-122.951	0.6	0.03	0.59	0.07	0.45	0.73	---	---	too low	---	---	TiO ₂
Elev. (ft)	0-90	197	197	115	115	16.5	0.3	16.62	0.47	15.7	17.6	too high	---	---	---	---	Al ₂ O ₃
Location	Signif. site G1, Quatsap Point delta	Tekiu Point Rd NW ^s	Tekiu Point Rd NW ^s	Thunder Ridge Way ^s	Thunder Ridge Way ^s	0.08	0.02	0.083	0.01	0.07	0.1	---	---	---	---	---	FeO*
	0.09	0.08	0.079	0.079	0.083	2.12	0.23	2.31	0.28	1.75	2.87	---	---	---	---	---	MnO
	2.676	2.39	2.31	2.34	2.36	4.66	0.35	4.79	0.4	3.99	5.59	---	---	---	---	---	MgO
	5.27	4.62	4.71	4.55	4.68	4.07	0.09	4.12	0.12	3.88	4.36	---	---	---	---	---	CaO
	4.30	4.3	4.33	4.25	4.16	2.27	0.1	2.04	0.16	1.72	2.36	too low	too low	---	---	---	Na ₂ O
	1.12	1.69	1.69	1.87	2.06	0.16	0.01	0.155	0.02	0.11	0.2	too high	---	---	---	---	K ₂ O
	0.280	0.169	0.164	0.165	0.188	0.16	0.01	0.155	0.02	0.11	0.2	too high	---	---	---	---	P ₂ O ₅
Total	100	98.66	98.64	98.43	100												

MAJOR ELEMENTS NORMALIZED (XRF; in weight percent)

Sample ID	(11-81-M-0783)	53S179A	1-T-13	2-K-9-Bb	K-9-B	Average of 20 Whidbey Is. volcanic clasts (Polenz and others, 2005)	Standard deviation of 20 clasts (Polenz and others, 2005)	Average of 107 Glacier Peak dacite clasts from east and north of Whidbey Is. (Dragovich and others, 2005)	Standard deviation of 107 clasts (Dragovich and others, 2005)	Low bound: Glacier Peak average of 107 - 2 standard deviations	High bound: Glacier Peak average of 107 + 2 standard deviations	Is Quatsap Point pebble outside 2 standard deviation range for Glacier Peak source?	Is Tekiu Point Rd NW pebble (53S179A) outside 2 standard deviation range for Glacier Peak source?	Is Tekiu Point Rd NW pebble (1-T-13) outside 2 standard deviation range for Glacier Peak source?	Is Thunder Ridge Way pebble (2-K-9-Bb) outside 2 standard deviation range for Glacier Peak source?	Is Thunder Ridge Way pebble (K-9-B) outside 2 standard deviation range for Glacier Peak source?	
Latitude	47.649	47.57945	47.57935	47.5854	47.5854							too high	too high	too high	too high	too high	
Longitude	-122.906	-122.959	-122.96	-122.951	-122.951							too high	too high	too high	too high	too high	
Elev. (ft)	0-90	197	197	115	115							---	---	---	---	---	
Location	Signif. Site G1, Quatsap Point delta	Tekiu Point Rd NW ^s	Tekiu Point Rd NW ^s	Thunder Ridge Way ^s	Thunder Ridge Way ^s							too high	too high	too high	too high	too high	
TRACE ELEMENTS (XRF; in parts per million)																	
Ni	45	44	45	36	43	19.4	3.35	18	5	8	28	too high	too high	too high	too high	too high	Ni
Cr	37	34	33	32	31	19.4	4.97	18	5	8	28	too high	too high	too high	too high	too high	Cr
V	83	75	74	72	81	83.6	7.96	81	12	57	105	---	---	---	---	---	V
Ga	20	18	18	19	19	17.4	0.76	17	1	15	19	too high	---	---	---	---	Ga
Cu	23	13	13	17	22	7.94	3	10	4	2	18	too high	---	---	---	too high	Cu
Zn	62	55	54	55	59	57.4	3.01	57	6	45	69	---	---	---	---	---	Zn
TRACE ELEMENTS (ICP-MS; in parts per million)																	
La	Analysis pending at Washington State University Geoanalytical Laboratory			Not analyzed			14.54	18.2	0.79	16.02	1.23	13.6	18.5				La
Ce							29.84	35.3	1.41	31.23	2.65	25.9	36.5				Ce
Pr							3.8	4.04	0.15	3.47	0.53	2.41	4.53				Pr
Nd							15.05	16.1	0.59	13.83	2.15	9.53	18.1				Nd
Sm							3.15	3.56	0.12	3.08	0.5	2.08	4.08				Sm
Eu							0.91	1	0.03	0.92	0.15	0.62	1.22				Eu
Gd							2.75	3.22	0.11	2.75	0.45	1.85	3.65				Gd
Tb							0.41	0.51	0.02	0.44	0.07	0.3	0.58				Tb
Dy							2.4	3.09	0.11	2.64	0.44	1.76	3.52				Dy
Ho	Not analyzed			Not analyzed			0.48	0.63	0.03	0.54	0.09	0.36	0.72				Ho
Er							1.29	1.76	0.07	1.48	0.24	1	1.96				Er
Tm							0.18	0.26	0.01	0.22	0.04	0.14	0.3				Tm

Analysis pending at Washington State University Geoanalytical Laboratory	Not analyzed												Yb														
	Not analyzed													Lu													
	Not analyzed														Ba												
	Not analyzed															Th											
	Not analyzed																Nb										
	Not analyzed																	Y									
	Not analyzed																		Hf								
	Not analyzed																			Ta							
	Not analyzed																				U						
	Not analyzed																					Pb					
	Not analyzed																						Rb				
	Not analyzed																							Cs			
	Not analyzed																								Sr		
	Not analyzed																									Sc	
	Not analyzed																										Zr

Table E3. New whole-rock chemical analyses for 15 basalt bedrock samples from the Brinnon quadrangle. For additional whole-rock chemical data from complementary locations within the map area, see Glassley (1974). Sample locations are noted as geochemistry sample sites on the map. Analyses by ALS Chemex, N. Vancouver, BC, Canada. Major oxides were determined by X-ray fluorescence (XRF) and trace elements by inductively coupled plasma mass spectrometry (ICP-MS). The laboratory states that accuracy is 5% for major element oxides (unnormalized) and 10% for trace elements. Fe₂O₃ represents total iron; LOI, loss on ignition. Rock types determined per TAS classification as presented in Le Bas and others (1986). (See also Fig. E2.) Major element variation is modest (45.0–52.9 wt % SiO₂, 1.7–2.5 wt % TiO₂, 5.7–8.6 wt % MgO, 0.58–0.44 Mg # (molar Mg/(Mg+Fe)). Greater variation is seen in the concentrations of both compatible and incompatible trace elements (for example, 60–340 ppm Cr, 80–580 ppm Sr, 9–18 ppm Nb). All of these lavas display slight light rare earth enrichment (2.0–4.1 La/YbN) and negligible Eu anomalies (0.95–1.07 Eu/Eu*). On tectonic discrimination diagrams, these rocks have trace element affinities of both mid-ocean ridge and intraplate lavas (Fig. E3). Cr and MgO concentrations show a general decrease from north to south (this table and Fig. E4), whereas incompatible elements (for example, Hf, Nb, V, K₂O) show the opposite trend. All samples with compositions outside the basalt range (see also Fig. E2) came from south of the Duckabush River. The spatial distribution of the chemical trends suggests flows in the southern portion of the Brinnon quadrangle are, on average, more differentiated than those in the northern portion.

Analytical Method – XRF (major oxides)														
			Unnormalized											
Site name (from north to south)	Geochemistry site	Rock type	SiO ₂	Al ₂ O ₃	Fe ₂ O ₃	CaO	MgO	Na ₂ O	K ₂ O	TiO ₂	MnO	P ₂ O ₅	LOI	Total
			(%)	(%)	(%)	(%)	(%)	(%)	(%)	(%)	(%)	(%)	(%)	(%)
Rocky Brook Crescent	G2	basalt	46.6	14.6	11.9	9.2	8.3	3.3	0.37	1.98	0.15	0.17	3.0	99.6
Mount Turner	G3	basalt	45.6	13.6	15.6	9.5	6.5	3.9	0.03	1.96	0.17	0.24	3.2	100.4
Green Hill	G4	basalt	46.1	14.5	11.2	9.8	7.2	4.2	0.31	1.59	0.17	0.15	4.5	99.6
Green Hill	G5	basalt	47.1	14.4	12.7	10.6	7.6	2.8	0.31	1.80	0.20	0.16	2.3	99.9
lower Dosewallips valley – south side	G6	basalt	47.6	14.3	11.6	10.6	7.3	3.1	0.31	2.20	0.19	0.21	2.6	100.1
Duckabush River	G7	basalt	46.0	14.6	11.8	10.4	6.8	2.9	0.50	2.21	0.16	0.22	2.9	98.5
south of Duckabush River – west	G8	basalt	47.5	15.0	12.5	11.5	7.0	2.7	0.23	1.89	0.17	0.18	1.5	100.0
Fulton Creek North	G9	basalt	46.5	14.4	12.9	10.7	6.4	3.5	0.38	2.00	0.19	0.20	3.0	100.1
south of Duckabush River – center	G10	basalt	47.8	13.7	12.7	9.9	6.7	3.5	0.23	2.42	0.18	0.25	2.4	99.8
upper McDonald Creek	G11	basaltic trachyandesite	51.1	12.4	11.1	8.8	5.8	4.7	0.45	1.85	0.19	0.26	1.9	98.6
Fulton Creek south	G12	basalt / picobasalt	41.7	14.3	13.7	14.0	5.6	1.0	0.12	1.88	0.17	0.27	6.7	99.3
south of Duckabush River. – east	G13	basalt	44.5	15.0	13.7	11.8	5.5	2.8	0.26	2.26	0.24	0.23	3.5	99.8
lower McDonald Creek 1 (upper flow)	G14	trachybasalt	49.9	13.0	11.3	8.4	6.3	4.8	0.15	2.19	0.24	0.22	2.8	99.3
lower McDonald Creek 2 (lower flow)	G15	basalt	45.6	14.4	14.1	11.2	5.7	2.9	0.16	2.37	0.20	0.24	2.3	99.1
South Fork Fulton Creek	G16	basalt	48.1	13.3	12.8	9.2	6.3	3.8	0.08	2.38	0.24	0.22	3.3	99.7

		XRF (major oxides)												Orig. Total
		Normalized to 100% Anhydrous											LOI	
		SiO ₂	Al ₂ O ₃	Fe ₂ O ₃	CaO	MgO	Na ₂ O	K ₂ O	TiO ₂	MnO	P ₂ O ₅	(%)		
Geo-chemistry site	Rock type	(%)	(%)	(%)	(%)	(%)	(%)	(%)	(%)	(%)	(%)	(%)	(%)	
G2	basalt	48.2	15.2	12.3	9.5	8.6	3.4	0.38	2.05	0.16	0.17	3.0	99.6	
G3	basalt	47.0	14.0	16.1	9.8	6.7	4.0	0.03	2.02	0.18	0.24	3.2	100.4	
G4	basalt	48.4	15.2	11.8	10.3	7.5	4.4	0.33	1.67	0.18	0.16	4.5	99.6	
G5	basalt	48.2	14.7	13.0	10.9	7.8	2.9	0.32	1.84	0.20	0.17	2.3	99.9	
G6	basalt	48.9	14.6	11.9	10.9	7.5	3.2	0.32	2.26	0.20	0.22	2.6	100.1	
G7	basalt	48.1	15.2	12.3	10.9	7.1	3.0	0.52	2.31	0.17	0.23	2.9	98.5	
G8	basalt	48.2	15.2	12.7	11.6	7.1	2.7	0.23	1.92	0.17	0.18	1.5	100.0	
G9	basalt	47.9	14.8	13.3	11.0	6.6	3.6	0.39	2.06	0.20	0.21	3.0	100.1	
G10	basalt	49.1	14.1	13.0	10.1	6.9	3.6	0.24	2.49	0.18	0.26	2.4	99.8	
G11	basaltic trachyandesite	52.8	12.8	11.5	9.1	6.0	4.8	0.47	1.91	0.20	0.27	1.9	98.6	
G12	basalt / picrobasalt	45.0	15.4	14.7	15.1		1.1	0.13	2.03	0.18	0.29	6.7	99.3	
G13	basalt	46.1	15.6	14.2	12.2	5.7	2.9	0.27	2.35	0.25	0.24	3.5	99.8	
G14	trachybasalt	51.7	13.4	11.7	8.7	6.5	5.0	0.16	2.27	0.25	0.23	2.8	99.3	
G15	basalt	47.1	14.9	14.5	11.6	5.9	3.0	0.17	2.45	0.21	0.24	2.3	99.1	
G16	basalt	49.9	13.8	13.2	9.5	6.6	3.9	0.08	2.47	0.25	0.23	3.3	99.7	

		Analytical Method – ICP-MS (trace elements)															
Geochemistry site	Rock type	Ba	Ce	Co	Cr	Cs	Dy	Er	Eu	Ga	Gd	Hf	Ho	La	Lu	Mo	Nb
		(ppm)	(ppm)	(ppm)	(ppm)	(ppm)	(ppm)	(ppm)	(ppm)	(ppm)	(ppm)	(ppm)	(ppm)	(ppm)	(ppm)	(ppm)	(ppm)
G2	basalt	118	26.4	54	270	0.01	5.11	2.8	1.67	19	5.18	3.7	0.99	10.2	0.35	<2	11.9
G3	basalt	12	30.7	52	160	<0.01	6.06	3.6	1.69	24	5.71	3.5	1.34	13.1	0.54	2	9.9
G4	basalt	59	22.9	44	340	0.18	3.72	2.2	1.35	16	3.92	2.7	0.77	10.3	0.27	<2	10.4
G5	basalt	46	21.7	50	280	0.01	5.6	3.3	1.49	21	5.01	3.2	1.15	8.7	0.44	<2	9.2
G6	basalt	177	32.9	44	330	0.03	4.73	2.6	1.76	19	5.27	3.9	0.98	14.4	0.33	<2	15.2
G7	basalt	142	37.8	48	270	0.01	5.82	3.1	1.96	22	5.72	4.4	1.11	15.7	0.39	<2	17.9
G8	basalt	74	31.3	59	320	<0.01	6.55	3.7	1.89	25	6.05	4.0	1.27	13.0	0.47	<2	13.6
G9	basalt	82	28.5	47	140	0.05	5.36	3.0	1.62	19	5.17	3.8	1.08	11.7	0.40	<2	13.1
G10	basalt	81	32.9	45	230	<0.01	7.17	4.1	2.07	19	6.91	4.8	1.27	14.1	0.57	<2	14.5
G11	basaltic trachyandesite	64	24.5	41	120	0.03	5.26	3.2	1.66	10	5.33	3.5	1.13	11.1	0.42	<2	8.9
G12	basalt / picrobasalt	18	27.2	40	60	0.04	5.22	3.2	1.62	17	5.33	3.2	1.14	13.8	0.43	2	10.5
G13	basalt	26	31	55	90	0.03	7.1	3.8	2.04	22	6.57	4.6	1.39	12.4	0.53	<2	12.4
G14	trachybasalt	26	33.2	55	140	0.02	6.45	3.5	2.06	21	6.26	4.6	1.24	13.6	0.44	<2	15.0
G15	basalt	64	31.9	56	170	0.03	7.01	3.8	1.96	24	6.61	4.7	1.37	12.6	0.49	<2	12.2
G16	basalt	32	31.5	48	130	0.01	5.88	3.1	1.80	19	5.87	4.3	1.15	12.6	0.41	<2	14.4

		ICP-MS (trace elements)																
		Nd	Pr	Rb	Sm	Sn	Sr	Ta	Tb	Th	Tl	Tm	U	V	W	Y	Yb	Zr
Geochemistry site	Rock type				(ppm)	(ppm)	(ppm)	(ppm)	(ppm)	(ppm)	(ppm)	(ppm)	(ppm)	(ppm)	(ppm)	(ppm)	(ppm)	(ppm)
G2	basalt	18.8	3.79	4.2	4.71	1	299	0.8	0.82	0.82	<0.5	0.35	0.26	360	2	27	2.26	143
G3	basalt	17.9	3.99	0.8	4.77	1	81	0.6	0.98	0.92	<0.5	0.49	0.50	354	<1	38	3.34	128
G4	basalt	14.8	3.32	5.2	3.77	1	252	0.7	0.65	0.86	<0.5	0.30	0.21	301	<1	21	1.98	93
G5	basalt	15.0	3.05	3.4	4.14	1	163	0.6	0.83	0.73	<0.5	0.44	0.21	381	1	32	3.00	119
G6	basalt	21.1	4.72	2.7	5.21	1	360	1.0	0.83	1.28	<0.5	0.37	0.32	367	<1	25	2.44	130
G7	basalt	23.5	5.09	8.1	5.50	2	406	1.1	0.89	1.34	<0.5	0.41	0.39	385	1	30	2.59	179
G8	basalt	21.2	4.34	1.8	5.36	2	244	0.9	0.97	1.10	<0.5	0.50	0.30	430	1	36	3.23	164
G9	basalt	18.5	3.88	4.0	4.71	1	296	0.8	0.83	0.92	<0.5	0.41	0.23	367	1	30	2.61	142
G10	basalt	21.7	4.86	2.6	5.83	1	336	1.0	1.16	1.26	<0.5	0.58	0.32	478	1	39	3.42	177
G11	basaltic trachyandesite	17.5	3.71	6.5	4.87	1	314	0.6	0.87	0.86	<0.5	0.46	0.82	376	<1	31	3.01	121
G12	basalt / picrobasalt	19.1	4.21	1.5	5.02	1	145	0.7	0.86	0.92	<0.5	0.47	0.29	361	1	34	3.06	110
G13	basalt	21.9	4.42	7.9	5.83	1	584	0.8	1.04	1.11	<0.5	0.54	0.32	441	1	39	3.54	183
G14	trachybasalt	23.0	4.68	2.2	5.71	1	150	1.0	0.98	1.07	<0.5	0.45	0.31	453	1	34	2.91	179
G15	basalt	22.1	4.61	2.9	5.86	1	428	0.8	1.06	1.05	<0.5	0.52	0.31	462	1	38	3.41	187
G16	basalt	21.2	4.45	1.1	5.31	1	264	0.9	0.93	1.06	<0.5	0.42	0.31	416	1	31	2.70	166

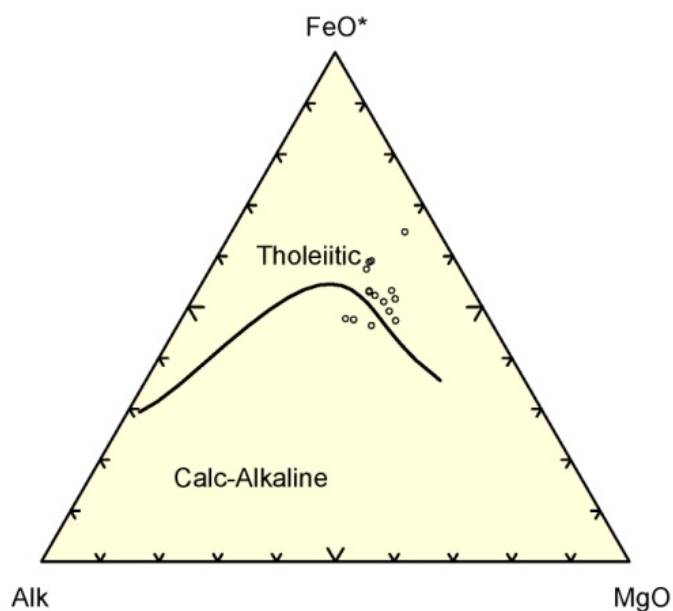


Figure E1. AFM diagram after Irvine and Baragar (1971) for basalt samples from the Brinnon quadrangle. Most of the lavas from the map area are tholeiitic basalt. The samples with calc-alkaline affinity are from south of the Duckabush River. (See distribution of samples from north to south within map area, as shown in Table E3.) This spatial ordering of calc-alkaline as compared to tholeiitic basalt lavas is part of a trend of chemical differentiation that increases from north to south of the Duckabush River and continues south into the Eldon quadrangle (Contreras and others, 2012a).

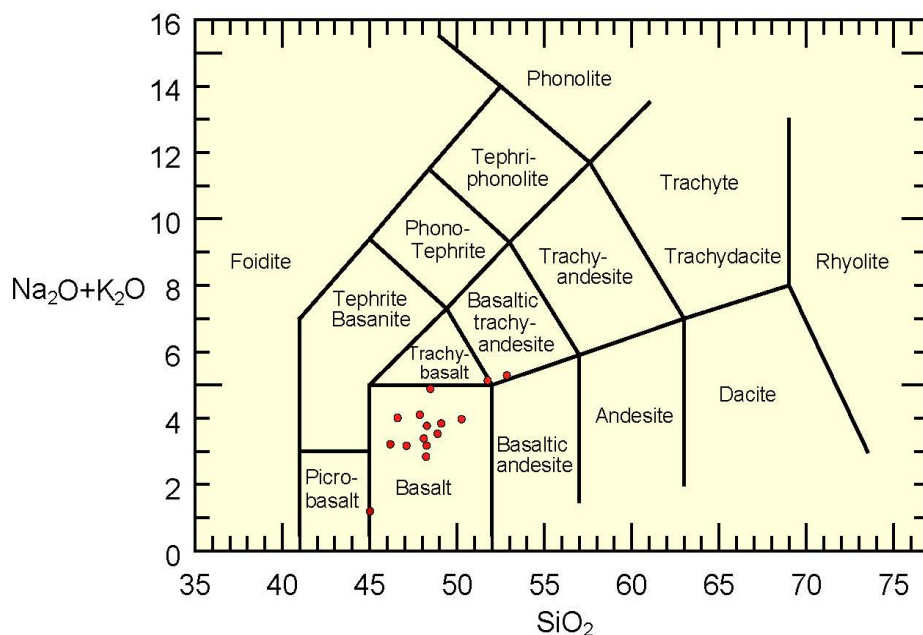


Figure E2. Total alkalis versus silica plot (Le Bas and others, 1986). Thirteen of 15 lava samples analyzed in mapping of the Brinnon quadrangle are basalt; one of these borders on picrobasalt. One sample barely meets trachybasalt composition. The sample that is most clearly not basalt is basaltic trachyandesite, and like the samples of trachybasalt and borderline picrobasalt, it is from south of the Duckabush River (see Table E3). This spatial ordering of basalt versus other lava types is part of a southward trend toward increasingly differentiated compositions observed among samples collected in the Brinnon quadrangle and farther south in the Eldon quadrangle (Contreras and others, 2012a).

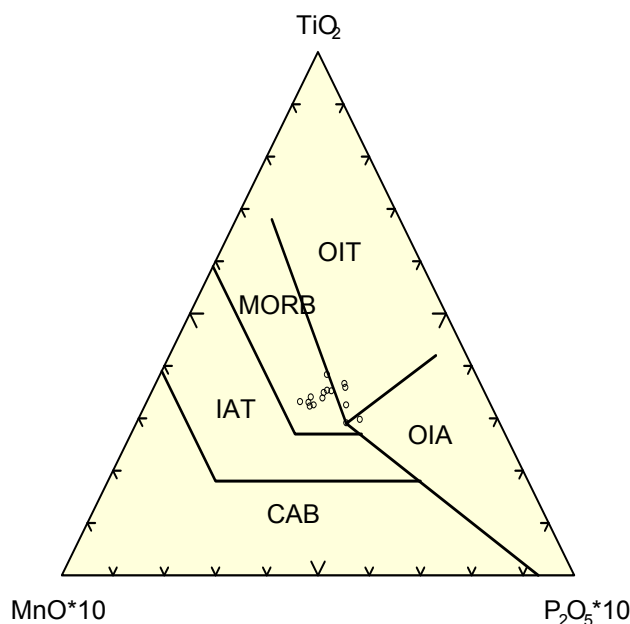


Figure E3. Tectonic discrimination diagram (Mullen, 1983) showing that Crescent Formation lavas from the Brinnon quadrangle display both MORB (mid-ocean ridge basalt) and OIT (ocean island tholeiites) affinities. OIA, ocean island alkalic; IAT, island arc tholeiite; CAB, calc-alkaline basalt.

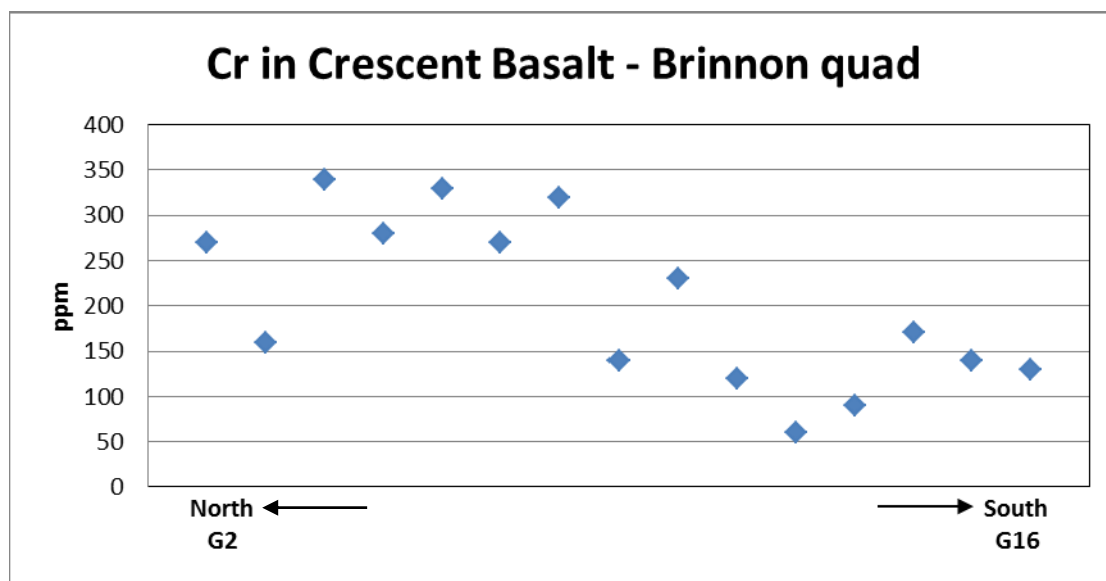


Figure E4. Plots of Cr and MgO content show that the Cr and Mg content decreases from north to south within the Brinnon quadrangle. The trend of southward-decreasing Cr and MgO content continues southwest into the Eldon quadrangle (Contreras and others, 2012a). The lower levels of some elements (Cr, Mg) are accompanied by higher levels of others (for example, Hf, La, MnO, P_2O_5 —Table E3), such that the chemical variability appears to reflect geographic rather than stratigraphic trends, although the paucity of reliable structural data make it difficult to establish a stratigraphy for the entire quadrangle, and the seemingly geographic trends we noted (this Fig. and Figs. E1 and E2) are not without exceptions.

